

# The Evolution of Applications, Hardware Design, and Channel Modeling for Terahertz (THz) **Band Communications** and Sensing: Ready for 6G?

By JOSEP M. JORNET<sup>®</sup>, Fellow IEEE, VITALY PETROV<sup>®</sup>, Member IEEE, HUA WANG<sup>®</sup>, Fellow IEEE, ZOYA POPOVIĆ<sup>®</sup>, Fellow IEEE, DIPANKAR SHAKYA<sup>®</sup>, Graduate Student Member IEEE, JOSE V. SILES<sup>®</sup>, Senior Member IEEE, AND THEODORE S. RAPPAPORT<sup>®</sup>, Fellow IEEE

ABSTRACT | For decades, the terahertz (THz) frequency band had been primarily explored in the context of radar, imaging, and spectroscopy, where multi-gigahertz (GHz) and even

Manuscript received 12 January 2024; revised 8 May 2024; accepted 31 May 2024. This work was supported in part by the National Science Foundation under Grant CNS-1955004, Grant CNS-2011411, Grant CNS-2117814, Grant CNS-2216332, Grant CNS-2037845, and Grant CNS-1909206; in part by the NYU Wireless Industrial Affiliates Program; in part by the Commission of the European Union CHIPS Joint Undertaking SHIFT Project under Grant 101096256; and in part by the Air Force Office of Scientific Research Award under Grant FA9550-23-1-0254. (Corresponding author: Josep M. Jornet.) Josep M. Jornet is with the Institute for the Wireless Internet of Things, Northeastern University, Boston, MA 02115 USA (e-mail:

Vitaly Petrov is with the Division of Communication Systems, KTH Royal Institute of Technology, 114 28 Stockholm, Sweden.

Hua Wang is with the Department of Information Technology and Electrical Engineering, ETH Zürich, 8092 Zürich, Switzerland.

Zoya Popović is with the Department of Electrical, Computer and Energy Engineering, University of Colorado Boulder, Boulder, CO 80309 USA. Dipankar Shakya and Theodore S. Rappaport are with the NYU Wireless

Research Centre, New York University, New York, NY 10012 USA. Jose V. Siles is with the NASA Jet Propulsion Laboratory, Pasadena, CA 91011

Digital Object Identifier 10.1109/JPROC.2024.3412828

i.jornet@northeastern.edu).

THz-wide channels and the properties of THz photons offered attractive target accuracy, resolution, and classification capabilities. Meanwhile, the exploitation of the THz band for wireless communication had originally been limited due to several reasons: 1) no immediate need for such high data rates available via THz bands and 2) challenges in designing sufficiently high-power THz systems at reasonable cost and efficiency, leading to what was often referred to as "the THz gap." Over the recent decade, advances on many fronts have drastically changed the THz landscape. First, the evolution from 5G- to 6G-grade wireless systems dictates the need to support novel bandwidth-hungry applications and services for both data transfer [i.e., eXtended Reality (XR), the Metaverse, and vast modeling needs of artificial intelligence (AI) and machine learning (ML)], as well as centimeter-precision sensing and classification (i.e., for standalone position location, vehicle-to-everything (V2X), or unmanned aerial vehicle (UAV) tracking). Second, substantial progress in THz hardware has been achieved, offering promise that the THz technology gap will be closed. Hence, THz-band wireless communication seems inevitably an essential part of the future networking technology landscape in the coming decades. To design efficient THz systems, the peculiarities of THz hardware and THz channels need to be understood and accounted for. This roadmap paper first reviews the evolution of the hardware design approaches for THz systems, including electronic, photonic, and plasmonic approaches, and the understanding of the THz channel itself, in diverse scenarios, ranging from common indoors and outdoors scenarios to intrabody and outer space environments. This article then summarizes the lessons learned during this multidecade process and the cutting-edge state-of-the-art findings, including novel methods to quantify power efficiency, which will become more important in making design choices. Finally, this article presents the authors' perspective and insights on how the evolution of THz systems design will continue toward enabling efficient THz communications and sensing solutions as an integral part of nextgeneration wireless systems.

**KEYWORDS** | 6G; channel modeling; hardware; sub-millimeter waves (mmWaves); terahertz (THz) communication.

#### I. INTRODUCTION

Each generation of the global cellphone industry has produced technological innovations that brought forth unexpected new use cases that exploit greater channel bandwidths and data rates. From the early days of analog cellular using 25- or 30-kHz channels in the first generation (1G) of cellphones, today's 5G cellphone standards (e.g., the 3rd Generation Partnership Project (3GPP)) exploit orthogonal frequency-division modulation (OFDM) and multiple-input—multiple-output (MIMO) antennas as well as massive MIMO and use many concatenated channel bandwidths, in 20-MHz chunks, allowing over 100 MHz of usable bandwidth with hundreds of megabits/second/user.

5G was the first global cellphone standard also to introduce spectrum above 6 GHz and ushered in the era of millimeter wave (mmWave) communications [1], where both frequency-division duplexing (FDD) and timedivision duplexing (TDD) can implement multi-gigabitper-second data rates in 200-MHz channel chunks and have enabled wireless carriers to implement both mobile services in urban cores with high pedestrian traffic loads and large venues (such as stadiums) as well as offering fixed wireless access (FWA) for homes and businesses in an unexpected and profitable way. Not all governments or carriers have adopted the mmWave bands, leading to varying opinions about the efficacy of mmWave. Yet, virtually, all global cellphone makers and infrastructure vendors now ship mmWave transceivers as part of their product offerings. In the unlicensed device arena, mmWave has found Wi-Fi adoption through IEEE 802.11ad and, more recently, IEEE 802.11ay, which theoretically supports up to 100-Gb/s data transfers. The move to greater bandwidths appears inevitable as more applications and services require massive data transfer rates.

Immediately after the release of 5G [2], both academia and industry started to envision what 6G should bring

to the users and, accordingly, what technologies will be needed [3], [4], [5], [6], [7]. The need to accommodate the exponentially growing number of wirelessly connected devices and their mounting data-rate requirements motivated the exploration of higher frequency bands, beyond mmWaves, including the sub-terahertz (sub-THz, 100–300 GHz) and terahertz (THz, 300–10 THz) bands [3], [8], [9], [10], [11], [12], [13], [14], [15], [16], [17], [18], [19].

This frequency range brings exciting opportunities to many applications across scales. The very small wavelength at sub-THz and THz frequencies (from 3 mm at 100 GHz down to 30  $\mu$ m at 10 THz) enables the development of miniature antennas that can be potentially embedded everywhere, from nanosensors in the Internet of Nano-Things (IoNT) to within computing processors for wireless network-on-chips (WNoCs). This is not possible at lower frequencies (e.g., sub-6 GHz and even mmWave, because of the much larger wavelengths). At the same time, the very small size of individual antennas allows for their integration in very large numbers over compact footprints. For a fixed antenna footprint (e.g., the size of current sub-6-GHz antennas on cellphones or in base stations), a sub-THz or THz antenna offers much higher directivity gains. This motivates, for example, the adoption of sub-THz frequencies for satellite communication networks, where the combination of high gain antennas in transmission and reception can facilitate closing the link compared to lower frequency bands. Across scales, this frequency range offers very large bandwidth (from tens to hundreds of gigahertz (GHz), if not more), which are only limited by hardware constraints or spectrum policy and regulations.

Much has been said about what these frequencies might and might not bring to the table, both in terms of communications and sensing (see [16, Table I] for a summary of the existing works). Still, today, five years before the expected release of 6G, one question remains: will THz technology be ready?

This article aims to answer this question by providing an updated view of two critical aspects, namely, THz hardware technology and channel modeling. The former determines the type and properties of the signals that can be adopted (in terms of frequency, bandwidth, and power, among others), the hardware-induced phenomena that can alter them (including amplitude and phase noises or nonlinear distortion) as well as the efficiency with which these can be processed at the transmitter (TX) and the receiver (RX). The channel models describe the phenomena affecting the propagation of such signals from the TX to the RX, which drastically depends on the application scenario (from indoors to outdoors, static or mobile, other emerging applications, and new opportunities). These two aspects set the cornerstone on which the communication techniques (e.g., time, frequency and phase synchronization, modulation and coding, and MIMO strategies) and the networking protocols (e.g., user discovery,

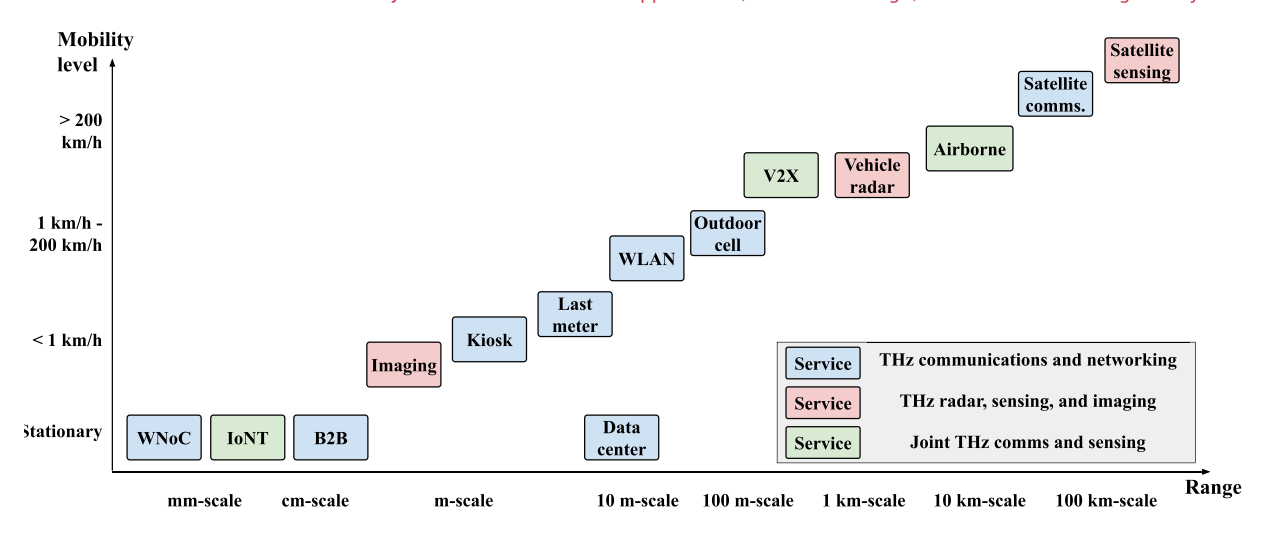


Fig. 1. Classification of major use cases for THz communications and sensing.

beam management, and mobility support) need to be developed.

The remainder of this article is organized as follows. In Section II, we describe the envisioned use cases for THz communications in 6G, classified not only as a function of the targeted communication range or use case but also the need to support different levels of mobility. This highlights the diversity in applications of THz technology while facilitating the identification of common aspects that guide the design of THz networks. In Section III, we describe the evolution of THz hardware technology, highlighting the trends in analog front ends, digital backends, and antenna systems. Compared to existing works, updated and largely quantitative data are provided concerning state-of-the-art THz device technologies. In Section IV, we present the key lessons learned from the extensive THz channel largely experimental modeling efforts in the last five years. In Section V, we discuss some of the critical aspects and opportunities relating to both hardware and channel modeling, as well as how these impact and enable the design of physical and link layer technologies. We conclude this article in Section VI.

# II. MAJOR USE CASES FOR THZ COMMUNICATIONS AND SENSING

Both the THz hardware design considerations and, especially, the THz channel modeling approaches heavily depend on the target environment and the target use case, as well as the carrier frequencies and form factors of the equipment allocated to such use. Therefore, in this section, we first present a harmonized vision of the major use cases for THz communications and sensing. Since supporting mobility is one of the key challenges for THz wireless networks, we arrange the use cases accordingly. We go from inherently stationary through low mobility all the way to highly mobile use cases, such as terrestrial wireless access, vehicular THz systems, and satellite-tosatellite THz communications. The proposed classification is also illustrated in Fig. 1.

The set of attractive use cases for THz communications and sensing is primarily determined by: 1) potentially (but not necessarily) millimeter-scale or sub-millimeterscale size of THz antenna elements (see Section III-B) and 2) potentially (but not necessarily) large system bandwidth in the order of up to several tens and even few hundreds of GHz. Another essential feature of the use cases here is that a combination of large-scale antenna systems with THz signal frequency leads to very directional transmissions that have both advantages (e.g., less interference) and challenges to overcome (beam alignment, node discovery, accurate position location, system clock synchronization, and so on). Whenever relevant, we point to the key distinct feature of THz communications for a discussed use case in the following.

# A. Stationary Use Cases for THz

1) Wireless Networks on Chips: The rapid increase in the characteristics, capabilities, and inline, and complexity of the computer chips challenge the scalability of the stateof-the-art approach to building computer platforms. Interconnecting all the essential chip components via either a shared wired bus or a set of wired buses going through the central hub becomes extremely challenging to implement. Modern central processing units (CPUs) already feature more than 16 computing cores, multiple co-processors (e.g., tailored to artificial intelligence (AI) or other specific applications), and several layers of shared cache memory, while graphics processing units (GPUs) or latest systemson-chip (SoCs) feature even more individual elements.

Hence, a novel use case arises, often referred to as WNoCs. The core idea is to replace multiple individual wired connections among small-scale elements on the chip with high-rate optical or THz wireless links through a shared medium [20], [21], [22]. Implementing such a system immediately raises novel challenges (design, fabrication, and control of nanoscale THz radio modules). At the same time, successful adoption of such an approach allows addressing the scalability problem of future chips by pushing the possible number of interconnected elements from a few hundred to many hundreds or even thousands of cores [23].

Simultaneously, WNoCs theoretically feature greater energy efficiency and a more compact design than traditional wired network-on-chips (NoCs). Both the inherently small antenna size and the large bandwidth play vital roles in this use case, enabling ultrahigh-rate short-range wireless links among many miniature THz radios on a chip. Importantly, from the wireless networking point of view, WNoCs present one of the simplest setups to control—a fixed number of connected nodes with full control of their behavior and no node mobility.

2) Board-to-Board Communications: This use case addresses the setup similar to the previous one but at a slightly larger scale. Specifically, board-to-board THz communications are envisioned as a possible alternative to space- and energy-consuming wired connections between the key elements in the computer, e.g., CPU-to-GPU, CPU-to-random access memory (RAM), and CPU-to-networking interface. Point-to-point THz links can replace or complement state-of-the-art solutions, including Peripheral Component Interconnect Express (PCIe), high-rate Universal Serial Bus (USB), and other wired options. More futuristic variations suggest integrating board-to-board THz communications with other essential elements, e.g., by utilizing cooling pipes between the CPU and the GPU as a waveguide for the THz signal [24].

There are two key distinct features of board-to-board THz communications from the previous use case, WNoCs. First, the communication normally happens at the centimeter, not millimeter (or even sub-millimeter) scale. Second, the communication system typically considers no more than a few (usually, two) connected elements, so there is no need for sophisticated control algorithms and protocols, as in the THz WNoC. Similar to the previous item, both small-scale THz antennas and large THz bands are essential enablers for this use case. Notably, the size requirements are less strict than for the WNoC, making not only THz, but sub-THz, or even mmWave radios applicable.

3) Data Center Links: Building THz-enabled high-rate wireless links in the data center is a further extrapolation of the previous use case (detailed in Section II-A2) to an order of magnitude larger distances. Specifically, the data center use case suggests interconnecting different server racks using point-to-point wireless THz links instead of Ethernet or optical fiber cables. This use case may sound counterintuitive to some, as the data center is a perfect example of stationary deployment, where wired connections have an advantage. However, the envisioned replacement of rack-to-rack wired links with high-rate and low-latency wireless

analog relaxes multiple restrictions essential for the data center layout (e.g., placement of racks in the room) and even cooling system design [25], [26], [27].

THz wireless links for data centers are also one of the key motivating use cases for the recently published IEEE standard for sub-THz connectivity, IEEE 802.15.3d–2017, and its upcoming revision just approved in 2023 [28]. The wide bandwidth is the essential property of THz communications, while the scale already allows for larger and relatively simple horn or lens-type THz antennas (see Section III-B).

4) Fronthaul/Backhaul: The last but definitely not least stationary use cases for THz communications are wireless fronthaul or wireless backhaul for 5G-Advanced and, especially, upcoming 6G cellular networks [3]. By design, multiplexing several (tens) of high-rate mobile access links (e.g., mmWave) into a single wireless link requires an order of magnitude greater bandwidth than only the THz band or optical systems can offer. Meanwhile, sub-THz and THz links are relatively robust to adverse weather conditions [29], [30], [31], which gives them a notable advantage from the reliability point of view.

Similar to the data centers above, the large bandwidth of the THz signal is the essential feature for the required high data rates, while the use of large-scale antenna systems on both sides addresses the spreading loss issue. Tentatively, wireless fronthaul/backhaul data links are likely one of the first use cases for THz communications to be adopted in 6G-grade networks.

# **B.** Low-Speed Mobility

1) Nanosensor Networks: One of the first use cases originally considered for wireless communications in the THz band is related to data exchange between microscale and nanoscale machines [32], [33]. These envisioned interconnected small-scale robots are to perform various tasks ranging from environmental sensing up to in-body medical invasions. The proposal partially stems from an earlier concept of the Internet of Things (IoT) pushing it further to the so-called IoNT [34].

The miniature (millimeter-scale or sub-millimeter-scale) size of THz antennas and attracted THz transceivers is the key inherent property of THz communications making it not only suitable for this use case, but even further, making it one of only a few possible communication methods at this scale (together with, e.g., optical wireless systems, molecular communications, and bacterial nanonetworks) [35].

2) Imaging: Historically, THz imaging was one of the first-ever use cases for THz wireless systems. Specifically, THz radiation is used to identify materials composing the scanned object, as different materials show different electromagnetic signatures (e.g., frequency-dependent transmissivity or reflexivity) when illuminated by the THz signal. Introduced and implemented several decades ago

(e.g., THz communication systems are still in the prototype stage today), THz imaging facilitates efficient and reliable scanning in many areas. These include, among others, luggage and postal mail screening, and 2-D and 3-D biological and chemical examination [36], [37].

Importantly, THz radiation is nonionizing—not enough energy carrier per quantum to remove an electron from the atom or molecule. Therefore, it is notably safer in practical scenarios (not fully safe though [38]), especially when it comes to medical scanning. Two major distinct properties of the THz band play vital roles for this use case: 1) large bands available (hence facilitating the scanner resolution) and 2) the fact that many common materials have notably different properties in reflecting, diffracting, and passing over the THz signal. Last but not least, the THz signal better penetrates certain obstacles (e.g., human skin) than optical signals, making it a promising option when it comes to multilayer 3-D scanning.

3) Kiosk Download/Data Shower: Another low-mobility use case for THz communications is typically referred to as one of the three similar terms: 1) kiosk download; 2) data shower; and 3) information shower [39], [40]. While the exact definitions of these vary from source to source, the general idea is almost the same. A kiosk (or a data/information shower) is an ultrasmall (a few meters in coverage or less) and, importantly, an ultrahigh-rate wireless cell that allows quasi-instant downloads/uploads of huge chunks of data (data rates of tens/hundreds of gigabits to a few terabits per second).

The core idea of this proposal is to complement the existing coverage-centric wireless networks (microwave or even recent mmWave ones) with strategically placed highrate THz data showers, thus allowing the users to exchange large amounts of cached data when in their range. Such locations may be the entrance of the metro station or a large shopping mall, an airport corridor, a busy intersection, or any other place with a high volume of humans passing per minute. While these few short-range showers are not able to completely replace existing networks, they can assist them notably by offloading a significant portion of heavy traffic [41]. Here, the large bandwidth of the THz signal is the main properly facilitating high-rate data exchange but simultaneously limiting the coverage of the THz data shower.

4) Last-Meter Interconnect: The last-meter THz connection is a variation of the THz kiosk for office or onbody environments. This use case suggests applying THz connectivity as the last hop between a distant remote server and the user terminal. Specifically, a single 1-m range THz cell (backed to the office wired network) can replace several Ethernet wired connections in a typical office desk or cubicle, e.g., desktop, laptop, and highresolution display, among others [42].

A more futuristic version of this use case describes a set of wearable (or eventually implantable) devices interconnected with THz wireless links, thus featuring extremely high rates and ultralow latencies [34]. These formed wireless personal area networks (WPANs) will include but are not limited to smart glasses (e.g., eXtended Reality (XR) [43]), on-body or in-body sensors, and even (eventually) Internet-to-brain and brain-to-Internet interfaces [44]. Similar to the previous use case, the high rates and low latencies are enabled primarily by wide THz bands, while the same wideband nature of transmissions limits the coverage of these envisioned THz WPANs.

# C. Medium-Speed Mobility

1) Femto Cells: THz-enabled ultrahigh-rate femtocells and/or THz wireless local area networks (WLANs) present a decisive use case for mobile THz communications. Specifically, an evolution of state-of-the-art IEEE 802.11ad/ay WLANs operating at 60 GHz is envisioned at the next Wi-Fi development cycle within 6G or 6G-Advanced timeline. In parallel, the design of cellular-controlled indoor sub-THz/THz cells is of interest to further boost the performance of cellular wireless networks indoors [3], [16].

This setup presents one of the most challenging use cases for THz communications to implement, as both the complex wireless channel with a lot of potential obstacles (furniture pieces, human bodies, walls, and so on) and unpredictable mobility of the user terminals (e.g., smartphones or XR glasses) must be overcome. Importantly, not only canonical macroscale mobility (large-scale movements of the user terminal) should be accounted for but also microscale (or so-called small-scale) mobility comprising unpredictable shifts and rotations of the device itself. It has been shown that such rotations often lead to unexpected misalignment of the narrow THz beams, thus compromising network reliability and performance. Similar to the above, wideband THz signals enable highrate data exchange, while large-scale (thus directional) THz antenna systems are needed to maintain the desired coverage of several (tens of) meters.

2) Microcells: This use case presents a futuristic extension of the previous one, suggesting true THz radio to be used for cellular access links (50-200-m coverage). While it has been experimentally shown that wideband THz signals can be reliably received from a large distance of up to several kilometers [45], maintaining more than 100-m coverage for mobile THz access links is a challenge, as such distances will inherently demand even narrower THz beams. Consequently, all the supporting control algorithms and protocols must be capable of operating over narrow (less than a few degrees) THz beams. While there are several promising solutions presented in this area recently [46], [47], [48], [49], the set of unsolved research problems to address remains large. These include reliable, efficient, and low-overhead beam tracking algorithms; fast node discovery protocols; novel interference management techniques; and intelligent time-frequency-space resource allocation solutions, among others. Still, a theoretical possibility to leverage an order of magnitude larger bands than those available at mmWave frequencies makes this use case tempting to continue research and engineering activities.

3) Automotive Radars: Utilizing THz signals for automotive (e.g., vehicle-mounted) radars is the second sensing-centric use case in our list. In contrast to THz imaging discussed above, automotive radars primarily target revealing the relative distance to the target and the relative velocity of the target, not the target's composition [50]. Modern vehicle manufacturers already integrate up to a dozen sensors into their latest models, from ultrasonic parking sensors through mmWave/sub-THz cruise radars to optical cameras to monitor the surroundings. Selected prototypes of autonomous driving vehicles get equipped with light detection and ranging (LIDAR) solutions, which are effectively "light-based laser radars."

While existing mmWave and sub-THz cruise radars already enable decisive applications, such as adaptive cruise control and semi-autonomous driving, further development of these systems using wider true THz signals will notably contribute to their angular and distance resolution [51]. Pulse-based radars and frequency-modulated continuous-wave (FMCW) radars are two widely spread approaches to estimating the distance and velocity of the target [52]. The first approach primarily relies on the round trip time of the reflected/scattered radar signal to estimate the distance, while the Doppler shift in the signal frequency will reveal the relative velocity. FMCW-type radars achieve a similar goal by comparing the received signal with its original shape in time and frequency domains. Here, both the narrow THz beam and the wide bandwidth of the THz radar signal naturally contribute to the performance of the THz-enabled automotive radars.

4) Vehicular Communications: In parallel to improving automotive radars, the THz community is currently exploring the possibility of partially reusing selected elements (e.g., THz antenna arrays) for THz vehicle-to-everything (V2X) communications. While one may argue that there is typically not enough traffic generated by a single vehicle to deploy a high-rate THz link, this is not always true. First, there are use cases, where a single THz vehicle-toinfrastructure connection may relay several active mobile links between user devices in the car (smartphones, tablets, XR glasses, and so on) and in-vehicle entertainment systems [53]. Hence, instead of serving several mobile links, the network only has to serve one, while the vehicle-mounted access point (AP) serves the rest. This usage scenario is especially practical for public transport, where, e.g., the entire bus or the entire tram/train coach can be multiplexed into a single THz access link [54].

Another decisive application motivating THz V2X is autonomous collective driving. Latest studies show that cooperation among the vehicles is one of the factors both: 1) simplifying control of the vehicle swarms and 2) improving the system performance. For instance, a group of connected vehicles can drive at high speeds on a highway with very low distance between each other, thus increasing

the road capacity. For this scenario, wideband THz signals enable high rates and low latencies, while using steerable directional beams facilitates little to no interference with other THz-capable cars, pedestrian users, and infrastructure nearby. Notably, connected smart vehicles are also one of the promising scenarios for joint THz communications and sensing, where the same hardware components are used for both radar sensing and data exchange [55].

# D. High-Speed Mobility

1) Connectivity for Airborne Nodes: The list of use cases with high mobility of nodes starts with exploiting THz communications for airborne nodes. These include both human-operated airplanes and unmanned aerial vehicles (UAVs) [56]. Within the first group, one of the primary targets is to improve connectivity to passenger airplanes. A commercial passenger airplane is a very expensive device whose cost may easily exceed \$100 million. A one-way ticket for a transatlantic flight is over several hundred U.S. dollars for economy and up to several tens of thousands for business and first class.

Despite these costs, a flying airplane is currently one of the world's worst connected places, with no more than a couple of megabits per second available per passenger over existing Ku-band (12–18 GHz), K-band (18–27 GHz), and Ka-band (26.5-40 GHz) (if all the passengers get connected). Improving this situation with mobile THz communication links between an airplane and a low-Earth orbit (LEO) satellite or between an airplane and the ground network (either directly or through another airplane) is a decisive practical usage scenario. Another vector of interest comes from primarily military-type use cases-connecting two or more airplanes, drones, or other flying objects (e.g., missiles) into a single low-latency THz network. While wideband THz signals are good for bandwidth-hungry data exchange, highly directional THz transmissions also facilitate covert and secure airborne communications.

- 2) Satellite Remote Sensing: Remote sensing is historically one of the first groups of use cases associated with THz radio systems that debuted decades ago. Until now, the U.S. National Aeronautics and Space Administration (NASA) has been the creator of some of the highest power THz front ends [57]. Today, there are dozens of satellitebased THz sensors deployed already and more currently in development due to several major reasons [58]. First, as discussed above in relation to THz imaging, the band is very useful for multilayer imaging of different objects. A combination of these unique properties with the wideband of the THz signal and low interference with Sun radiation makes THz waves good candidates for remote sensing of planets. Furthermore, as water is one of the key absorbers at THz frequencies, there are many satellite-based THz sensors deployed around the Earth used for environmental sensing, including weather forecasts.
- *3) Low Earth Orbit Satellite Communications:* Stemming from the previous two, THz band communications present

an attractive alternative to mmWave and optical systems when it comes to satellite communications (especially, building large-scale mega constellations at the LEO). On one side, the THz band features larger bands than those currently used in the K-band or around for satellite-toairplane and satellite-to-ground connectivity [60], [61]. On the other side, relatively wider THz beams demand less precision from the beam-pointing mechanism than laser-based intersatellite crosslinks [62]. Importantly, THz signals are also less affected by the Sun radiation and atmospheric turbulence than optical signals [63].

Last but not least, while mmWave bands may be too narrow for crosslinks and optical links may be not powerful enough to facilitate Earth-to-satellite connectivity, the THz band may serve as a sweet spot in the middle [62], [64]. Prospective LEO satellites may be equipped with a single THz radio module for crosslinks, access links, and environmental sensing (e.g., using joint communications and sensing) instead of three separate radio modules (optical, mmWave, and THz), all operating at different bands and consisting of different radios. Hence, the stringent space and weight restrictions for spacecraft become less crucial with the use of THz wireless systems.

# III. EVOLUTION OF THZ HARDWARE TECHNOLOGY

The THz band was called the THz gap for decades because of the lack of device technologies to support communication and sensing applications at these frequencies. However, the situation is much different today. As we summarize below, there are multiple solutions to realize the critical hardware building blocks of a THz wireless system. These include the analog front ends, the antenna systems, and the digital signal processing (DSP) backends. Importantly, while many times developed independently by the communications and the sensing communities, these hardware blocks are fundamentally the same, and their joint design can only benefit communications, sensing, and joint communication and sensing applications.

# A. Analog Front Ends

The analog front end generates, modulates, filters, and amplifies signals at THz frequencies with multi-GHz bandwidths. The key performance metrics of a front end include the frequency bands of operation, modulation bandwidth, transmission power, RX sensitivity, amplitude and phase noise, and power efficiency.

There are three approaches to building THz front ends.

1) Electronic Approach: This approach pushes the limits of the devices and designs used in microwave and millimeter-wave frequency systems toward the THzband frequencies. The general challenges for THz highperformance solid-state front ends are mostly caused by the limited performance of electronic devices at the THz frequency spectrum, including limited device power gain,

output power, energy efficiency, noise figure (NF), and the circuit footprint. Moreover, there are considerable challenges in accurately measuring the characteristics of the fabricated electronic THz front ends with micrometer and sub-micrometer device areas and contact geometries. Considering the device parasitics, signal transitions, and power limitations in THz circuits, detailed calibration and measurement techniques become paramount to ensure the desired performance of THz devices [65]. In such direction, new capabilities, such as the multiuser THz measurement facility at New York University (NYU), New York, NY, USA, provide no-cost open access to test and measurement hardware and capabilities for collaborating researchers across the United States [66].

a) Silicon technology: Currently, most commercially complementary metal-oxide-semiconductor (CMOS) technologies offer device unit gain at frequencies  $f_{\text{max}}$  around 300–350 GHz, which is subject to further degradation due to layout parasitics. Considering a perfectly neutralized differential device pair, the resulting device unilateral power gain (U) is inversely proportional to the square of the operating frequency, and its unit-gain frequency  $f_{\text{max}}$  stays almost the same as that of the native device [67]. Therefore, most reported CMOS amplifiers operate at 150 GHz or below, with a theoretically limited device gain of 6 dB per stage before accounting for any passive matching network losses. Although there are reported techniques to boost the device gain beyond U [68], [69], [70], [71], tradeoffs with device stability and bandwidth typically need to be made.

While the CMOS device power gain is one root cause for its limited THz performance, the device Johnson limit [72] also predicts the diminishing output power capability of CMOS devices at THz frequencies, which matches well with reported data based on Eidgenössische Technische Hochschule (ETH) power amplifiers (PAs) Survey [59] (Fig. 2). Furthermore, the limited device gain and output power capability require more amplifier stages in cascade and in power combining, both degrading the energy efficiency (Fig. 3). In addition, the low device power gain directly compromises the achievable NF, while using more amplifier stages to achieve the target gain results in large front-end transceiver circuit footprints that exceed the standard  $\lambda/2$  antenna array grid size beyond 150 GHz (Fig. 4) [73].

Recently reported D-band CMOS/CMOS silicon-oninsulator (SOI) PAs mostly adopt class-A biasing to maximize the device gain at the expense of energy efficiency [70], [74], [75]. They achieve saturated output power ( $P_{\text{sat}}$ ) of +18 dBm, 1-dB gain-compression output power (OP<sub>1 dB</sub>) of +14 dBm, and peak power added efficiency (PAE) of 10%-14%. However, the modulation energy efficiency is typically below 2%. Recent D-band CMOS/CMOS SOI low noise amplifiers (LNAs) report NF of 4.7-6 dB and often employ device gain boosting techniques [76], [77], [78], [79].

Jornet et al.: Evolution of Applications, Hardware Design, and Channel Modeling: Ready for 6G?

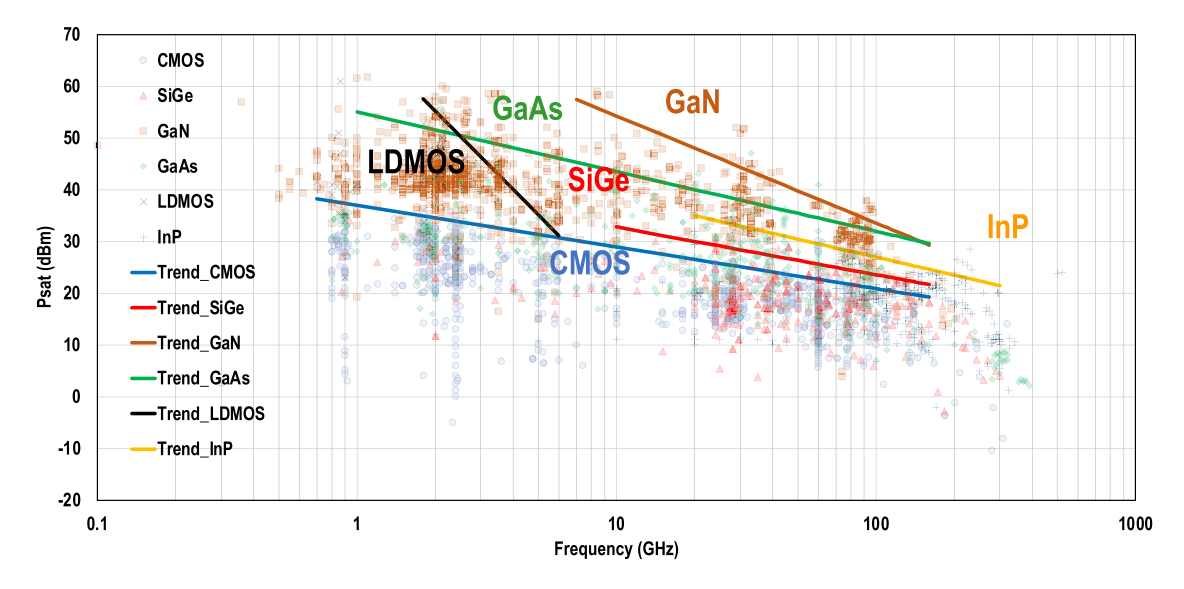


Fig. 2. PA survey. Saturated output power versus frequency for different electronic front-end technologies [59].

In addition, for frequency generation for D-band wireless systems, the popular approach is to generate the local oscillator (LO) signal first at lower mmWave frequency and then multiply the LO frequency up to the D-band by frequency multipliers [80], [81], [82], [83], [84], which exhibits a balanced tradeoff of phase noise, frequency tuning range, and power consumption. At the system level, multiple D-band TX and RX designs have been reported with typical 10%-14% carrier bandwidth to support highspeed modulations [80], [84], [85], [86], [87], [88], [89], [90], [91], [92]. While the single-channel TX/RX performance is fundamentally governed by the PA/LNA performance, realizing 2-D scalable arrays for practical mobile wireless applications (e.g., TX/RX co-channel or dual-polarization) will entail other challenges on circuit footprint and thermal density. They will require other techniques, such as heterogeneous integration.

To operate close to or beyond device  $f_{\rm max}$ , one should resort to device nonlinearity and harmonic generation, leading to even poorer output power capability and energy efficiency. For example, CMOS circuits are used to build

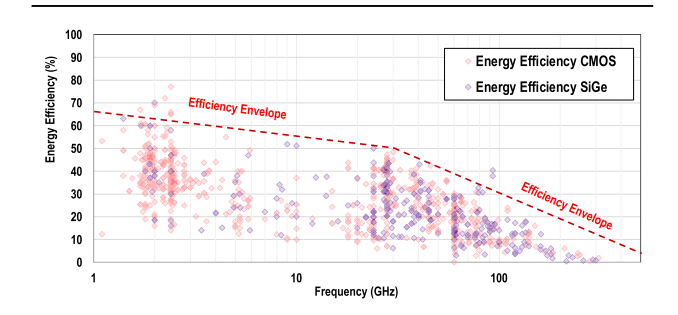


Fig. 3. Energy efficiency of CMOS and silicon germanium (SiGe) integrated circuits (ICs).

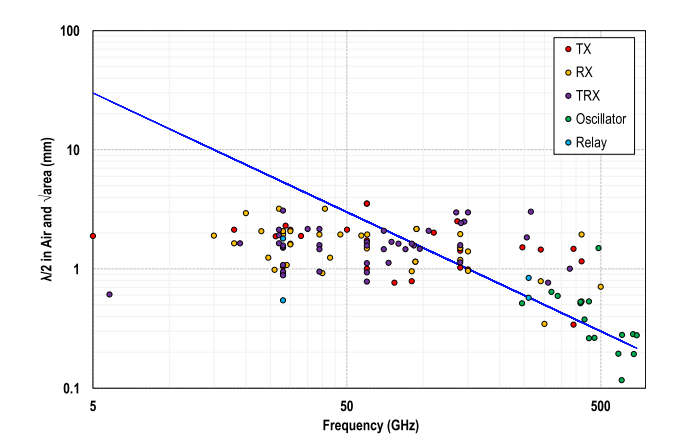


Fig. 4. Chip element area for different circuits/system types.

systems at frequencies approaching 300 GHz, but with transmit power in the order of only 1 mW, capable only for short-range communication and sensing [93]. Another option to increase the performance of siliconbased devices, such as the CMOS devices described this far, is to explore the integration of silicon with other materials in new structures, such as with advanced SiGe heterojunction bipolar transistors (HBTs) from Global-Foundries, STMicroelectronicsics, and IHP. Such devices can achieve  $f_{\text{max}}$  over 500 GHz and are less sensitive to layout parasitics. However, similar design tradeoffs still exist, showing the limitation of silicon-based devices and the need for III-V compound technologies and heterogeneous integration. On the other hand, silicon-based technologies offer unparalleled integration density, signal processing, and controls/reconfigurations, which are essential for THz front ends and systems.

b) III–V semiconductor technologies: Although siliconbased circuits have shown high-frequency operation with

medium-level power from power-combined devices, for watt-level power, III-V semiconductors are needed. To increase the power output to tens of milliwatts, amplifiers based on III-V semiconductor materials can be utilized [94].

High-electron-mobility transistors (HEMTs) using indium gallium arsenide (InGaAs) developed in the 1980s [95] allowed a path for mmWave solid-state amplifiers and other components at the W-band (75-110 GHz). The power of an individual solid-state device at high frequencies is limited, and traditional binary corporate combining is dominated by loss before substantial power levels can be reached. Spatial power combining techniques introduced using gallium arsenide (GaAs) technology include, e.g., a 272-element lens array using the same number of GaAs mmWave ICs (MMICs) with a total output power of 36 W at the V-band (40–75 GHz) [96]. With research over the past few decades bringing wide bandgap semiconductors to the stage, gallium nitride (GaN) has been improving high-frequency performance with operating frequencies in the hundreds of GHz [97], [98]. Although vacuum tubes have demonstrated several hundreds of kilowatts at the W-band, e.g., [99], they are narrowband and require large power supplies and magnets. The wide bandgap of GaN and high associated operating voltages make it the semiconductor of choice for high-power solid-state TXs. The silicon carbide (SiC) substrate additionally offers good thermal properties compared to GaAs and silicon. A number of recent millimeter-wave GaN processes with gate lengths in the 20-90-nm range have shown high performance across V- and W-bands [100], [101], [102], [103].

Various GaN processes on SiC substrates currently achieve cutoff frequencies above 200 GHz. For example,  $f_T$ up to 275 GHz is shown in a 40-nm GaN on SiC HEMT process [101]. Power densities as high as 3 W/mm are shown at the W-band in GaN on SiC [101]. Device efficiency is also increasing at the W band, with 45% PAE reported for a 3-W/mm high-power device at 94 GHz, while the same device can reach 56% PAE with an output power density of 780 mW/mm [101]. The highest published GaN Wband TX, intended for an active denial weapon, produces around 6.8 kW [104] by spatially combining over 8000 GaN-on-SiC MMIC PAs, each with over 1 W of power and PAE >20% around 93 GHz. This approach is modular and therefore scalable.

Advanced GaN processes also achieve minimum NFs below 2 dB at the W-band [100], [101] and about 7.6 dB above 100 GHz [105]. The ability to design with multiple gate lengths allows for increased complexity, such as low noise/high gain stages followed by high linearity stages in a single LNA [106]. A comprehensive review of GaN MMICs up to the 110-GHz range is given in [107]. Despite the impressive results in GaN, the lowest NFs and the highest frequencies of operation are obtained in indium phosphide (InP) (see [94], [108], [109], and [110]).

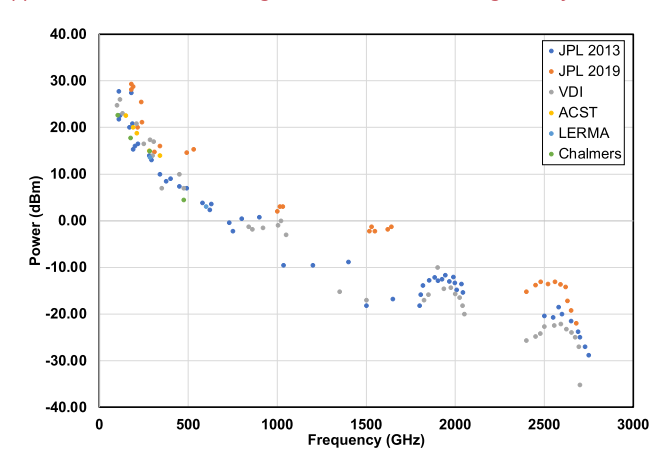


Fig. 5. Schottky-diode-based frequency multipliers survey. Output power versus frequency achieved by different groups, including the NASA JPL, Virginia Diodes Inc. (VDI), ACST. LERMA at the Observatoire de Paris/C2N, and Chalmers University

GaN MMICs with various functionality through W-band have been demonstrated. This includes switches with high IP3 (over 30 dBm) and isolation (over 40 dBm) [111], continuous 90° and 10° phase shifters from 50 to 110 GHz [112], active frequency doubling and tripling with conversion gain [113], active circulators [114], and a 50–110-GHz amplifier–isolator with 60-dB isolation [115].

III-V semiconductor materials can also be utilized to build different types of diodes with applications in THz signal generation and detection, including Schottky diodes, resonant tunneling diodes (RTDs), and impact ionization avalanche transit times (IMPATTs). For example, GaAs-based Schottky diodes are commonly used as frequency multipliers and mixers in frequency upconverting and downconverting chains [116]. For example, in [57], frequency-multiplied THz sources providing up to ten times more output power at room temperature than the previous state-of-the-art are prototyped at 180 GHz, 240 GHz, 340 GHz, 530 GHz, 1 THz, and 1.6 THz. Using such technology, a frequency tripler with 200 mW of output power at 225 GHz is built and utilized to establish a 2-km-long link carrying multi-gigabit-per-second (Gbps) in [45]. A survey of the most recent works demonstrated based on this technology is shown in Fig. 5.

2) Photonic Approach: In this approach, the limits of devices and architectures used in optical communication systems are pushed down in frequency toward the THz band. The devices in this category are very diverse, ranging from electrically pumped to laser pumped, pulsed wave to continuous wave, and many even include electronic and/or plasmonic components. While offering faster, lower phase noise, and high Q-factor, this approach has a few disadvantages such as lower power, difficulty in implementation, cryogenic temperature operation, bulky, low efficiency, and minimal tunability, and often only emits short pulses.

An example of an electrically pumped optoelectronic device is the quantum cascade laser (QCL) [117], [118], [119], a type of semiconductor laser with emissions through intersubband transitions in a repeated stack of alternating semiconductors, forming multiple quantum well heterostructures. Laser-pumped devices [120] include difference-frequency generations (DFGs) [121], optical rectification, optical parametric oscillators, and photoconductive antennas (PCAs) [122]. The DFG achieves optical heterodyne signal generation with a beam combiner of two optical lasers of different frequencies,  $\omega_1$  and  $\omega_2$ , followed by a photomixer to output a single laser beam of frequency  $\omega_2 - \omega_1$ , in this case in the THz range.

PCAs [123] use laser pulses instead of continuous-wave lasers, which are incident on a highly resistive direct semiconductor thin film with two electric contact pads. The incident laser has higher photon energy than the semiconductor energy gap and is absorbed in the film, creating short-lasting electron–hole pairs until recombination.

3) Plasmonic Approach: This approach aims to leverage the properties of plasma waves and surface plasmon polariton (SPP) waves to build devices that intrinsically operate at THz frequencies. Among others, plasma waves—or oscillations of electrical charges in a material—at THz frequencies can be excited in an asymmetric plasmonic cavity formed in the 2-D electron gas (2DEG) channel of a HEMT, due to the so-called Dyakonov—Shur instability [124]. Such a transistor can be built with III–V semiconductor materials [125], [126], [127], [128], [129] and/or with 2-D materials such as graphene [130], [131].

Besides signal generation, the same structure can provide high-speed modulation of the generated plasma wave in frequency and amplitude [132]. Amplitude modulation is achieved by varying the dc bias current passing through the transistor channel. Alternatively, frequency modulation can be achieved by varying the gate voltage. In other words, this device can act as a direct amplitude or frequency upconverter from baseband or an intermediate frequency (IF) to THz frequencies. Moreover, direct phase modulation can be achieved by means of a tunable plasmonic waveguide built again with graphene [133]. In this setup, by varying the bias voltage of the plasmonic waveguide, the speed of the SPP wave can be changed, and accordingly, the phase at the output of the waveguide can be modulated. In addition to other on-chip graphenebased modulators [134], off-chip modulating structures based on graphene and other 2-D materials have been proposed [135]. These structures interact with the radiated signals and should not be confused with on-chip structures integrated with the TX that interact with the signal before being radiated. In this sense, they are closer to the antenna systems described in Section III-B.

In broad terms, the size of plasmonic devices is proportional to the plasmonic wavelength, which is generally much smaller than the free-space wavelength of a signal at the same frequency. The parameter that measures the ratio between the free-space and plasmonic wavelengths is the

plasmonic confinement factor and can easily be between 10 and 100 in graphene [136]. As a result, the generated power of graphene-based plasmonic devices is generally very low (approaching 1  $\mu$ W). However, their very small footprint supports both their embedding in nanomachines to enable the nanoscale applications of the THz band and their integration in larger numbers to build highly functional on-chip arrays [137]. Compared to the electronic and photonic approaches, the plasmonic approach has been much less explored, resulting in a high-risk, high-reward opportunity [138].

#### B. Antenna Systems

As in any wireless communication system, antennas are needed to convert on-chip signals into free-space propagating electromagnetic waves at the TX and perform the reciprocal function at the RX. Moreover, antenna systems can also be found along the channel, acting as surfaces that can manipulate electromagnetic radiation in different ways (e.g., as fixed or programmable reflectors, focusing transmission lenses, and polarization filters, to name a few), as we further elaborate in Section V. The key performance metrics of an antenna system include radiation efficiency, directivity gain, and beamwidth.

Fundamentally, classical antenna theory remains valid at THz frequencies, but there are some caveats. First, the very small wavelength of THz radiation leads to tiny THz antennas. For example, a resonant dipole antenna at 1 THz is approximately 150  $\mu$ m and has the conventional donut-shaped radiation diagram. Correspondingly, in reception, the tiny size of the dipole results in a very small effective area or aperture, leading to very high spreading losses (more in Section IV). Making the antenna larger to increase its effective area automatically leads to a more directional radiation pattern. This is why directional antennas are commonly used at THz frequencies. For example, horn antennas or even small dish antennas with gains ranging from 20 to 55 dBi are commercially available today.

Another way to achieve high gain is by building antenna arrays. Antenna arrays offer the advantage of being able to program the radiation diagram by controlling at least the phase, if not also the amplitude, at every antenna. The very small size of individual THz antennas allows their dense integration in very small footprints. Besides the radiating elements, an array needs to integrate at least the control elements (e.g., phase shifters/time delays and amplitude controllers). Moreover, suppose that the antenna needs to support MIMO communications. In that case, it will require numerous front ends, up to one per antenna, but usually one per subgroup of antennas [139]. Currently, designs with up to 16 streams, each feeding either one or a small group of antennas, have been demonstrated when following an electronic approach [140].

In addition to antennas, lenses can be utilized to control the radiated THz signals. Lenses can be used to focus the signal at a distance or to generate different types of wavefronts, such as nondiffracting Bessel beams [141], [142]

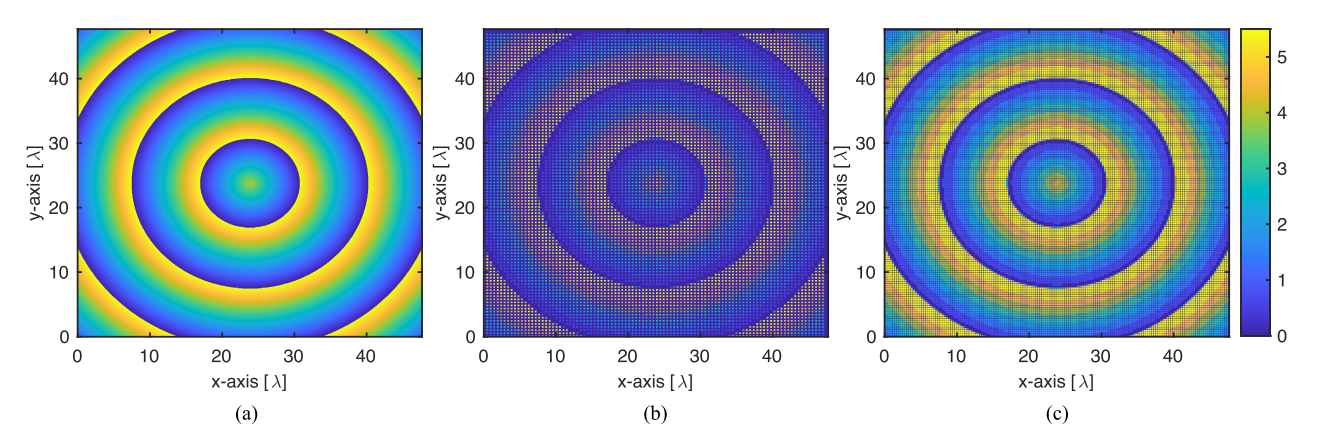


Fig. 6. Generation of a Bessel beam through (a) an ideal lens, (b) conventional antenna array with  $\lambda/2$  element size and spacing, and (c) plasmonic antenna array with  $\lambda_{spp} = \lambda/20$  element size and spacing. Note that at 300 GHz,  $\lambda = 1$  mm, and thus, the theoretical footprint of these structures is only 5 cm.

and self-accelerating Airy beams [143]. Moreover, besides dielectric lenses, these functionalities can also be implemented using metasurfaces. Metasurfaces are arrays of meta-atoms or custom-designed electromagnetic elements whose size is much smaller than the wavelength [144]. In the same way that an antenna array is a discretized, programmable representation of a larger antenna, a metasurface is the discretized, potentially programmable representation of lens. Nonetheless, the discretization process introduces losses too. For example, in Fig. 6, the resulting wavefronts when generating a Bessel beam through a continuous lens, an array with elements every  $\lambda/2$ , or a metasurface with elements every  $\lambda/20$  are shown.

1) Note on Plasmonic Structures: When adopting the plasmonic approach to build analog front ends, plasmonic nanoantennas are needed [145], [146], [147], [148]. The main advantage of plasmonic nanoantennas is that they are significantly smaller than the wavelength. While this leads to a smaller effective area, it also opens the door to their very dense integration [149], [150], [151]. Moreover, due to the small size of the plasmonic front end itself, arrays of integrated plasmonic front ends and plasmonic nanoantennas can be made [137]. The fact that their size is smaller than the wavelength and that each array element provides its own power and independent phase and amplitude control results in the possibility of performing not only beamforming as with metallic antenna arrays but also wavefront engineering as with programmable metasurfaces. All these structures can be designed to operate in transmission, reception, or reflection [152].

2) Role of Reflecting Surfaces: As mentioned at the beginning of this section, in addition to the TX or the RX, electromagnetic structures, including antennas, arrays, lenses, and metasurfaces, can be placed along the channel to enhance the propagation of THz signals. In particular, intelligent reflecting surface (IRS) and reconfigurable intelligent surface (RIS) have become extremely popular across all frequencies [153], [154], [155]. At lower

frequencies, IRS can increase the spectral efficiency of existing networks [156], [157], [158], [159]. As we move toward sub-THz and THz frequencies, IRS becomes a critical technology to increase coverage and, among others, overcome the impact of blockage by engineering nonline-of-sight (NLoS) paths around obstacles [160], [161], [162]. Focusing on the hardware aspects, IRS at THz frequencies are usually based on programmable reflect arrays or programmable metasurfaces [163]. At lower frequencies, p-i-n diodes or varactors are utilized to change the reflection phase of each reflectarray or metasurface element. However, the design and fabrication of such devices are challenging at THz frequencies. In [164], a GaN-based reconfigurable metasurface has been designed and experimentally demonstrated. The metasurface implements an array-of-subarrays architecture with subwavelength spacing and 1-bit control per subarray and supports wavefront engineering at 0.34 THz. Alternatively, the use of graphene as the tunable element in THz IRS has been theoretically proposed [165], [166]. Finally, nonreconfigurable reflecting surfaces with minimal complexity have been recently demonstrated [167], [168].

3) Discussion on the Near Field of Large Radiating Structures: At this point, it is relevant to remember that the far field of a radiating structure depends on the antenna size as  $2D^2/\lambda$ , where D is the largest antenna dimension [169]. Accordingly, for example, the far field of a 20-cm antenna array at 120 GHz starts at 32 m. The far field of the same antenna size at 1.05 THz (i.e., the center frequency of the first absorption-defined transmission window above 1 THz) does not start until 280 m. If, instead, a much larger antenna structure, such as a 2-m dish or surface, is used, the far field of the same communication and sensing system at 120 GHz and 1.05 THz is 3.2 and 28 km, respectively. As a result, in many applications, THz communications and sensing will happen within the near field of the antenna. Unfortunately, traditional beam management strategies, which imply a plane wave assumption with a uniform phase and where the spreading

Jornet et al.: Evolution of Applications, Hardware Design, and Channel Modeling: Ready for 6G?

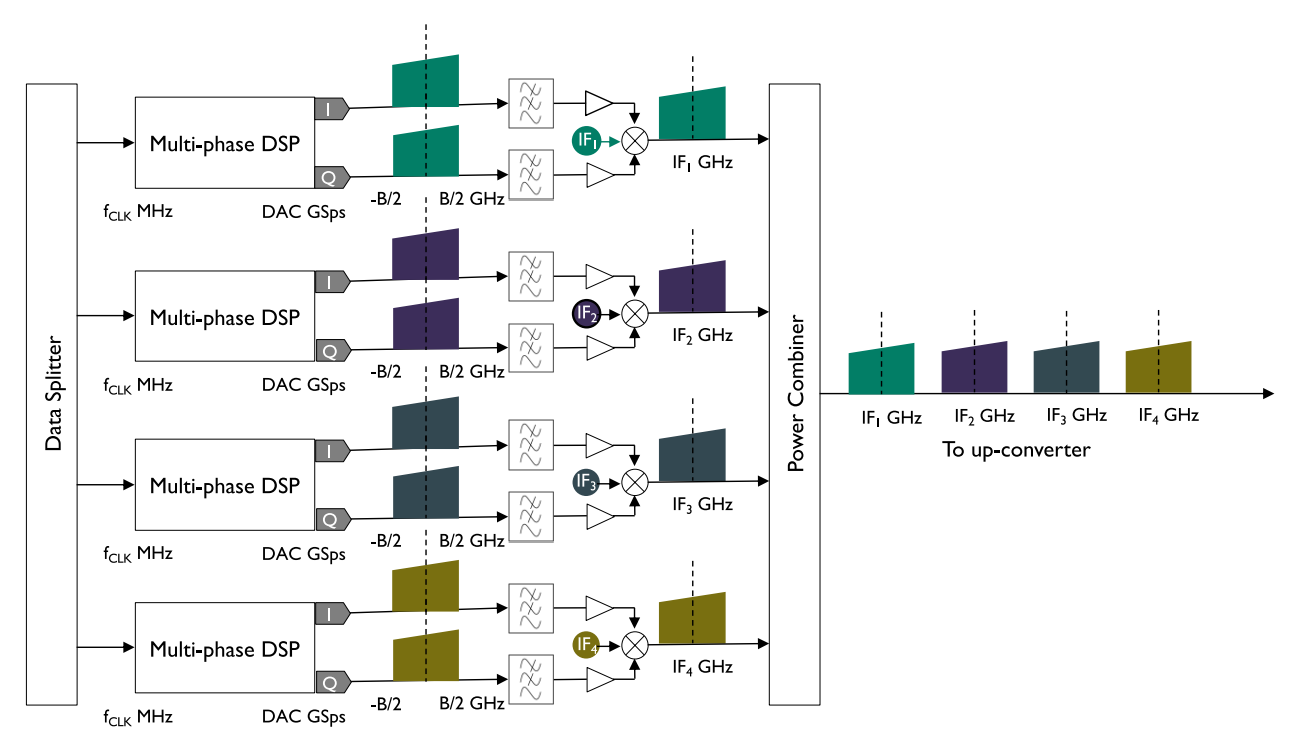


Fig. 7. Multichannel DSP engine. A large bandwidth is digitally processed by splitting it into four broadband channels, and each channel can be processed in real time through a multiphase parallel design.

effect results in a Gaussian intensity [169], including those proposed for THz systems, are inaccurate [170].

#### C. Digital Backends

The main motivation to move to THz frequencies is its enormous bandwidth. Accordingly, a DSP engine able to exploit such bandwidth is needed. The key performance metrics include the sampling frequency and the sampling resolution.

Common to optical (wired and wireless) systems, a major bottleneck in the DSP engine is posed by the digitalto-analog converters (DACs) and the analog-to-digital converters (ADCs). As of today, data converters with sampling frequencies of up to 256 gigasamples-per-second (GSaps) can be found in commercial laboratory-grade equipment (e.g., Keysight M8199B). As per the Nyquist sampling theorem, such data converters could operate with signals with analog bandwidths of up to  $B = f_s/2$ , i.e., ideally close to 128 GHz. Practically, this is less than that (e.g., 80 GHz for the aforementioned device). While this is remarkable, the size, cost, and thermal requirements of such data converters limit their application to very specific setups, far from what a handheld device could afford. In addition, such very high sampling frequencies come at the cost of lower resolutions (e.g., 8 bits). A lower resolution leads to a higher error vector magnitude (EVM) right from the start, i.e., at the TX, and thus impacts the performance of high-order modulations.

Alternatively, highly parallelized DSP engines are being developed. In particular, separate subchannels can be

independently processed by much slower data converters and (orthogonally) multiplexed in frequency (see Fig. 7) [171]. Following this approach, we have recently demonstrated what, as of today, is the fastest software-defined radio (SDR) platform for wireless communications, able to process in real-time 8 GHz of bandwidth by multiplexing four 2-GHz-wide channels in frequency [172]. More specifically, this platform leverages the state of the art in Radio Frequency (RF) system-onchip (SoC) (RFSoC) and multiphase processing strategies to generate four parallel IQ streams with a baseband bandwidth of 1.25 GHz each, and an IF multiplexing/demultiplexing custom board to generate/split a single ultra-broadband signal with 8 GHz of bandwidth. Multiphase processing strategies are needed to match the difference in speed between the field-programmable gate array (FPGA) clock (e.g., up to 512 MHz in the most optimistic case) and the speed of the data converters on the RFSoC (e.g., a few gigasamples-per-second (GSps)).

# D. Optimizing Power Waste for Green Communications

Green information and communication technology (ICT) has become an important topic for sustainable development as energy demand for ICT soars, and the impacts of anthropogenic climate change become unavoidable [173]. ICT is estimated to consume over one-fifth of the global electricity supply by 2030, equivalent to 8000 TWh/year [174]. While limiting the growth of ICT is impractical,

Table 1 Summar	of the State	of the Art in T	Hz Front Ends

Property	Technology Pathways				
	Electronic	Photonic	Plasmonic		
Frequency Range	Easily < 1 THz, potentially up go 10 THz	Easily > a few THz, potentially < 1 THz	1 THz and up		
Bandwidth	Up to tens of GHz	> 10 GHz	> 10 GHz		
Transmit Power	100s of mWs < 300 GHz, few mWs at 1 THz	<10 mW	<1 mW		
Amplitude and Phase Noise	High	Low	Unknown		
Technology Maturity	High	Medium	Low		

improving efficiency and reducing power waste of communications devices certainly alleviates the energy burden. As 6G networks are estimated to serve millions of connected devices with smaller cell sizes, potentially leveraging the THz and sub-THz spectrum, a metric to quantify the power waste of individual devices, cascaded communication systems, and networks is urgent. The power waste factor, W, denotes the amount of wasted power for devices, systems, or networks [175], [176]. W can be used by circuit and system designers to make informed decisions about design choices for devices based on the amount of power wasted. W provides an intuitive mathematical framework for power waste that closely resembles Harald Friis' NF [177].

In particular, the power waste factor, W, for any device or linear system (including any active or passive device or channel) is defined as

$$W = \frac{P_{\text{consumed,path}}}{P_{\text{signal}}} \tag{1}$$

where  $P_{\text{consumed,path}} = P_{\text{signal}} + P_{\text{non-signal}}$  [178], [179]. The waste factor efficiency,  $\eta W$ , is the reciprocal of W. The additive wasted power of any device is given by

$$P_{\text{waste}} = P_{\text{non-signal}} = (W - 1) P_{\text{signal}}$$
 (2)

where it is clear that any power that is consumed but not used in the output signal (e.g.,  $P_{\mathrm{non-signal}}$ ) is wasted power. Considering a cascade of N devices having a device gain, G and W for the device cascade can be obtained as [176]

$$W = W_N + \frac{(W_{N-1} - 1)}{G_N} + \frac{(W_{N-2} - 1)}{G_N G_{N-1}} + \dots + \frac{(W_1 - 1)}{\prod_{i=2}^N G_i}.$$
(3)

With W, circuit designs can be optimized for minimal energy waste; individually optimized devices can then be cascaded to build energy-efficient communication systems that form an energy-optimized network together. Furthermore, W can also be implemented in data centers to minimize their power waste [176]. The wasted power determined using W can be elegantly tied to the data rate delivered by the cascaded communication system to evaluate the consumption efficiency factor (CEF)

[175], [180]. Mathematically, the CEF is expressed as

$$CEF \left[ \frac{bps}{Watt} \right] = \frac{Data \ rate \ [bps]}{W \times Output \ Signal \ Power \ [Watt]}$$
 (4)

and signifies the data throughput per watt of power consumed. Therefore, with W and CEF, minimizing energy waste becomes an intrinsic part of the design process, creating the pathway for realizing the "green-G" future.

# E. Summary

In a nutshell, these are the key takeaways relating to the state of the art in THz device technologies.

- 1) THz analog front ends are quickly becoming available. Today, electronic frequency-multiplied transceivers at sub-THz frequencies are commercially available for equipment testing, while the research community shifts toward developing silicon/III–V heterogeneous systems, photonics, and, eventually, plasmonic-based configurations. A summary of the technologies is provided in Table 1.
- 2) The small wavelengths of THz signals enable the development of (sub) millimetric omnidirectional antennas as well as very high gain directional antennas with compact footprints (e.g., 20 dBi in 1 cm<sup>2</sup>). The latter can be in the form of fixed directional antennas (e.g., horn antennas, commercially available) or antenna arrays (still in development).
- 3) In addition to antennas, compact lenses and metasurfaces can be utilized to engineer the THz radiation at the TX, at the RX, and along the channel in the form of RISs. The main challenge today is to make such surfaces programmable at THz frequencies due to the challenges in developing tunable elements in this band.
- 4) While the main motivation to move to THz frequencies is the availability of larger bandwidths, today, one of the main technology challenges relates to the ability to digitally process them, mainly due to the cost, size, power requirements, and energy consumption of high-speed data-converters. This motivates both the adoption of largely parallelized signal processing techniques (e.g., multichannel systems), as well as the

- development of hybrid analog and digital processing techniques.
- 5) Across all the building blocks of a THz radio, energy efficiency becomes critical. The waste factor is a new metric that allows end-to-end optimization of energy consumption.

# IV. KEY LESSONS FROM THZ CHANNEL MODELING

#### A. Overview

Channel measurements and channel modeling for THz communications in various environments have been one of the primary research targets in the community until very recently. To date, hundreds of measurement- and simulation-based THz channel models have been presented in parallel to tens of analytical THz channel model studies [181], [182]. Because of the high close-in free-space path loss (FSPL) at greater frequencies (e.g., smaller wavelengths), virtually all propagation measurements and communications in the THz bands (perhaps with the exception of WNoC and IoNT) require directional antennas, from which omnidirectional channel models are created [183], [184]. Omnidirectional channel models are used by industry within standards bodies such as the 3GPP global cellphone standards body so that any antenna pattern may be implemented in simulation [185], [186].

Notably, as we argue in this article, the evolved understanding is that there will not likely be any single widely adopted THz channel model. Instead, there is a need to develop a range of THz channel models tailored to a specific use case and a particular propagation environment. The reason here is that while the physics of the THz wave propagation does not change much among the use cases, different distinct features of THz propagation have different weights when it comes to their contribution to the structure of the received signal. Therefore, it is more beneficial to work on a set of THz channel models for different use cases rather than aim to deliver a single unified model (with enormous complexity) that suits them all.

In the following, we briefly outline and review the latest findings in the field going from simpler to more complex setups that are potentially within the 6G timeline: outdoor THz links, indoor THz access, and vehicular THz systems. We also mention the specific use cases from the list above for which the given modeling approach is the most applicable. We start with reviewing outdoor setups, where the line-of-sight (LoS) THz path is the dominant factor determining the performance in Section IV-B. We then proceed with Section IV-C detailing the peculiarities of THz channel indoors. We later discuss vehicular THz setups in Section IV-D. The key takeaways are given in Section IV-E. Table 2 illustrates and complements our discussion.

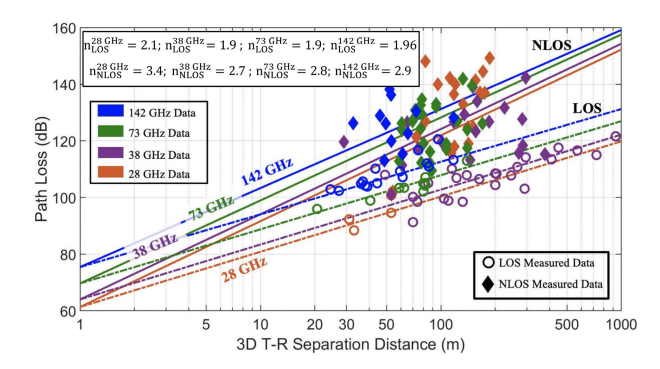


Fig. 8. Outdoor UMi omnidirectional CI path loss models with a reference distance of 1 m and without antenna gain [12]. The 28-, 73-, and 142-GHz measurements were conducted in New York and 38 GHz in Austin, TX, USA.

#### **B.** Outdoor THz Channel

The nonoccluded LoS THz channel typical for various outdoor environments is one of the most in-depth studies to date. During the last two decades, numerous measurement- and modeling-based studies have explored various aspects of outdoor THz channels. We aim to summarize the key findings from those given next. In brief, the impact of five different effects has been studied to date: 1) spreading loss; 2) molecular absorption loss; 3) molecular absorption noise; 4) scattering; and 5) diffraction [181].

1) Spreading Loss: Propagation path loss over distance is based upon the spherical spreading of the radiated wavefront (e.g.,  $1/d^2$ ) as modeled by H. Friis in the 1940s [187]. The distance-squared path loss is well known to represent free-space loss due to spreading, with "2" often referred to as the path loss exponent [39]. Today, the general understanding is that the spreading loss is the dominant factor when it comes to LoS outdoor sub-THz and THz channels contributing the most to the overall attenuation in the majority of conditions. This conclusion has been confirmed in various theoretical [188], [189], simulation-based [190], [191], [192], and measurementbased studies for a wide range of scenarios including urban microcell (UMi) [12], urban macrocell (UMa) [193], and rural macrocell (RMa) [194], among others [181], [195], [196], [197], [198], [199], [200]. Based on the close-in path loss model with a reference distance of 1 m, measurements conducted for UMi scenario in New York and Austin, TX, USA; Fig. 8 plots the path loss with distance at mmWave and sub-THz frequencies in LoS and NLoS [12]. The CI model characterizes the path loss behavior with a single parameter, the path loss exponent (n), beyond the free-space reference distance and was found to be the most robust using a vast range of measurement databases

<sup>1</sup>In addition to these five, outdoor THz channel may also feature nonnegligible impact of human-body blockage and the multipath components coming from, e.g., NLoS paths, reflected or scattered from buildings or other obstacles, as further discussed in Section IV-C.

across the mmWave and the sub-THz spectrums [201]. To overcome the increasing FSPL, wireless systems have adopted highly directional antennas and antenna arrays with narrow beamwidths at both ends of the link [17], [202]. As the physics of THz spreading is not principally different from lower frequencies (including mmWave), most of the measurement-based works agree on the fact that the average distance-dependent path loss exponent for sub-THz and THz channels is around 2 (with slight deviations depending on the scenario) [203], as illustrated in Fig. 8. Hence, the canonical FSPL equation originated by Friis holds for LoS THz propagation as well.

However, one essential element to highlight here is that the FSPL equation is based on the Friis transmission equation, which is only valid in the far field [169]. Therefore, the FSPL-based model is only valid for longrange stationary THz communications (e.g., for fronthaul and backhaul) employing small-scale horn or lens antenna. On the contrary, mobile THz communications for 6G- and 7G-grade wireless access links will likely utilize notably larger phased THz arrays or even leverage THz IRS [152], [162], [204]. The distinct feature of the latter is a nonnegligible near-field zone of the THz antenna system that can be comparable to the range of mobile THz communications, as discussed in Section III-B. The near-field region for commonly used THz antennas can be of tens to hundreds of meters or even more as we move to true THz frequencies. Such values are comparable to the coverage range of prospective THz outdoor cells and also exceed the target coverage range of indoor THz WLAN APs discussed further. The fact that the RX is in the near-field zone of the TX lowers the distance-dependent exponent far down from 2 and also leads to multiple research challenges summarized in Section V.

2) Molecular Absorption: The second key feature often mentioned in THz outdoor channel studies is the additional signal attenuation caused by molecular absorption. While molecular absorption loss is not exclusive to THz frequencies (e.g., some mmWave subbands, such as around 60 GHz, are notably affected as well), it can be orders of magnitude stronger than at lower frequencies [189]. Molecular absorption loss does not exist in a vacuum but in other environments typical for THz communications. Specifically, when the THz wave propagates through a gas, some portion of the wave energy gets converted into the kinetic energy of some of the environment molecules that have their resonant frequencies next to the ones of the THz wave itself [205]. The presence of molecular absorption loss: 1) makes THz channel (even in the simplest LoS case) frequency-selective and 2) adds an additional distance-dependent exponent to the aggregated path loss equation that notably complicates further analysis [206], [207], [208].

However, the impact of molecular absorption is of secondary importance and can be neglected in many typical use cases and environments under two important

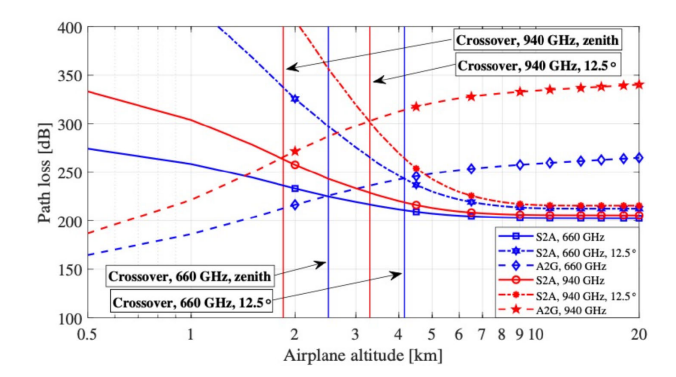


Fig. 9. Airplane THz communications measurements and results [209].

conditions. The first condition is that the entire spectrum of the transmitted signal lies within the so-called THz transparency window [210], [211]. For any sub-THz transmission, this one is fulfilled automatically, as the first transparency window is up to 540 GHz, while sub-THz transmissions are limited to 300 GHz [212]. The second important condition comes from the distance dependency of the molecular absorption loss. Here, it has been revealed both theoretically and experimentally that (under the first condition as well) the molecular absorption loss has an impact of less than 2 dB for any distance shorter than a few hundred meters. Therefore, the impact of molecular absorption can be ignored in the first-order analysis of sub-THz channels for outdoor cellular access, V2X, vehicular radars, and even short-range fronthaul and backhaul THz links. The only exception here is substantially wet weather (e.g., heavy rain) when an additional 2-3 dB should be subtracted from the received power value estimated by the THz channel model [30].

Airborne THz communications (including airplane-tosatellite links) are a special case for THz channel modeling. In particular, as THz molecular absorption is not only distance but also a pressure- and temperature-dependent variable, the value changes at different altitudes. As both higher temperature and greater pressure contribute to the THz molecular absorption loss, its value decreases rapidly with altitude (lower pressure and colder air). Specifically, THz molecular absorption loss becomes almost negligible at altitudes greater than 10 km making this effect not only distance—but also altitude-dependent. For selected THz subbands, this comes to an interesting tradeoff as recently revealed in [209] and illustrated in Fig. 9. Specifically, starting from a given altitude, a notably longer (e.g., 200 km) link between an airplane and an LEO satellite features lower loss than a comparable link between the same airplane and the ground station (no more than 10 km away).

Notably, molecular absorption in THz communications is not always an exclusively negative effect to avoid. In contrast, this effect can also be leveraged to, e.g., boost the secrecy and security of the data exchange over the

THz channel. Specifically, as discussed in [213], among other works, the transmission over the THz band can be limited in range by sensing the signal in the subband close to one or several "absorption lines"—frequencies features by a notably greater molecular absorption loss. Hence, if the separation distance between the TX and the RX is known, the TX becomes capable of "cutting" the message propagation beyond the RX, so any other nodes staying further away cannot reliably decode the message.

3) Molecular Absorption Noise: The third distinct feature studied for THz communications is the molecular absorption noise. This effect is caused by the fact that a fraction of the kinetic energy absorbed by the molecules from the THz signal is reemitted back to the environment as a standalone signal at the same/similar frequency as per the so-called emissivity of the channel [189], [205]. Canonical 5G-grade channel models typically decouple noise-related effects from channel-related effects, as most noise sources are present at the RX and are thus not part of the channel model itself. This is different for THz communications, as this specific type of noise—molecular absorption noise comes not from the RX but from the environment itself. It has been further revealed that this noise source is also correlated with the transmitted signal (e.g., greater transmit power leads to greater noise level) [214], [215]. Hence, accounting for the presence of molecular absorption noise properly is extremely challenging. For example, even the use of canonical Shannon capacity and signal-to-noise ratio (SNR) formulas implies that the noise is independent of the signal, which is no longer true at THz frequencies. The resulting analytical channel and interference models in the presence of molecular noise get notably more complicated compared to the ones in the very same setup but ignore this effect [208].

Fortunately, the total power of molecular absorption noise theoretically cannot exceed the power captured from the molecular absorption loss discussed above. Hence, the latest studies conclude that (while the molecular absorption noise is likely present in most of the setups) its contribution to the received signal power and shape is of secondary importance compared to: 1) spreading loss and 2) molecular absorption loss itself. Therefore, a common trend recently is to start ignoring this effect in complex first-order studies for the sake of analytical tractability [203], [216]. This choice is recommended for channel modeling targeting most practical THz use cases from Section II and most environments. While the accuracy is affected only slightly, the overall complexity of the analysis decreases dramatically, allowing for more sophisticated models to be built.

4) Scattering and Diffraction: The remaining two items related to THz channel modeling in open environments are scattering and diffraction. Both can be theoretically characterized by relatively complex expressions, as in, for example, in [217], among other works. The good news here is that scattering loss in THz communications (in

contrast to optical wireless systems) in typical homogeneous environments (e.g., air) is extremely low and can be ignored in first-order analysis in most conditions. Two exceptional cases here are: 1) adverse weather conditions (specifically, snow), where scattering from snow particles may lead to additional 5–8-dB losses and extra multipath created even in a pure LoS channel [29], and 2) scintillation/atmospheric turbulence effects. Therefore, as discussed further in [30], different THz channel models for the fronthaul/backhaul THz wireless link are needed for summer and winter conditions.

Regarding diffraction, the effect is especially visible when the THz signal meets a sharp object (e.g., a side of the building or furniture element). One of the essential findings here is that the THz link can be established even in partial blockage in the "obstacle's shadow" due to the diffraction effect [218]. However, this finding is primarily related to NLoS THz communications discussed in Section IV-C. On the contrary, diffraction from the environment molecules themselves (e.g., different molecules present in the air) is almost always negligible when it comes to THz channel modeling.

#### C. Indoor THz Channel

Another active area of research related to THz channel modeling primarily targets indoor THz channels. Indoor THz small cells or THz-empowered WLANs are among the target use cases and deployment scenarios for THz communications, as discussed in Section II. Complementing the findings on LoS THz propagation discussed above, indoor THz channel measurement and models primarily focus on the impact of the THz wave interaction with typical obstacles, such as building walls, furniture elements, and human bodies.<sup>2</sup>

1) Room Environment: Home or Office: Home or office is one of the most present environments when it comes to research works on indoor THz channels (both measurement-based and modeling-centric). Several key building blocks are needed to enable accurate THz channel modeling for indoor environments. The first one is an accurate and flexible THz LoS propagation model capturing all the essential features from the previous section. The second building block in an accurate characterization of the major objects present in the environment (particularly their penetration, reflection, and scattering properties at the frequencies of interest must be revealed).

Here, an extensive set of studies has been delivered at the early stages of 5G standardization for mmWave communications, specifically focusing on 26–30-GHz and 52–71-GHz frequency bands. The key findings from these studies are well summarized in earlier tutorials on

<sup>&</sup>lt;sup>2</sup>As noted in the previous section, selected findings on the humanbody blockage and reflection/scattering from building walls may also be relevant to outdoor THz channel models, e.g., for outdoor mobile access links.

mmWave indoor propagation [195], [219], [220]. After a decade of measurement and modeling of indoor sub-THz and THz communications, we may conclude that there is a great similarity between the mmWave and the THz channel when it comes to indoor environments [10], [221], [222]. For both frequency bands, the presence or absence of the LoS component is the primary factor determining the link performance. Furthermore, both bands feature strong reflections from flat surfaces, such as office desks and primarily walls, glass windows, and even ceilings [42].

The key difference of THz communications here is not qualitative but quantitative. Specifically, many typical indoor surfaces are good reflectors for low-mmWave signals (e.g., 28 GHz). Therefore, many indoor mmWave channel models assume them perfectly flat and act as reflectors with a certain loss of usually no more than a few decibels. The difference here comes from the fact that for sub-THz and especially true THz frequencies above 1 THz (hence, over 30 times shorter wavelength than at 28 GHz), the same typical home or office surfaces (e.g., a painted wall or a wooden door) are not flat anymore with nonnegligible roughness [223]. As an example, 142-GHz scattering measurements in [224] identified rough surfaces with the Rayleigh criterion [187] and found relatively high scattered power in nonspecular directions for incident angles below 30° for drywall. As the variations in the surface level become comparable to the sub-millimeter wavelength of THz communications, the reflected signal is weaker, while additional scattered signal copies are created. These scattered signals do not follow the law of reflection, so they propagate in many directions. Furthermore, these scattered components get reflected and scattered further from other objects in the environment, creating additional signal copies. Hence, while many mmWave models give sufficiently accurate predictions indoors by purely modeling LoS and reflected paths (e.g., via ray-tracing methods), an accurate channel model for THz communications benefits from also including at least the first-order scattered paths (TX-obstacle-RX) into the analysis [42].

2) Corridor and Data Center: The key peculiarity of indoor THz channel modeling for corridors is that a long corridor may act as a "waveguide" for THz signals. Notably, as the length of the corridor is typically at least several times greater than its width and height, the angle of departure (AoD) and angle of arrival (AoA) for most of the signal paths are relatively close to each other. This is a distinct feature of the corridor environment from a regular office or homeroom, where multipath comes from almost any angle due to pseudorandom reflection and scattering from the surfaces surrounding the TX and the RX. Therefore, many of these multipath copies of the transmitted signal will be successfully received even when using narrow-beam THz antennas. Hence, in contrast to an indoor setup that features occasional multipath that can be ignored in firstorder studies, the THz channel model for corridors must capture the multipath components coming at least from

the first- and second-order reflections, as they may be not notably weaker than the LoS component.

In general, modern channel models developed for THz communications in data centers (one of the distinct use cases for THz, as discussed in Section II) have large similarities to the ones used for corridors. This comes from the similarity of the environments and propagation conditions, as most data centers exploit corridor-based layouts with several rows of racks staying parallel to each other with a certain (usually fixed) separation distance. The key difference here comes primarily from the materials used for the server rack blocks (usually flat aluminum, steel, or plastic covers). Hence, a series of server racks acts similar to a flat wall with perfect reflection capabilities. As a result, the formed corridor may also act as a waveguide leading to the power delay profile (PDP) featuring a single strongest LoS component that comes first. The PDP continues by a few visible slightly weaker first- and second-order reflections followed by numerous higher order reflections and scattered components that are typically too much delayed to contribute to the received power of the given symbol and primarily contribute to the intersymbol interference (ISI) [225].

3) Human-Body Blockage: One of the essential features of mmWave and, especially, THz communications is substantial penetration loss when propagating through the human body. According to medical studies, up to 60% of the adult human body consists of water, which is a strong absorber of THz radiation. Consequently, the human-body penetration loss at mmWave, sub-THz, and THz frequencies ranges on the conditions (angle of incident, part of the body affected, beamwidth, and so on) but is in the order of 20–35 dB [226]. Such great losses not only challenge the overall average system performance (e.g., the capacity of the THz link) but also lead to frequent and unexpected outage events caused by dynamic human-body blockage.

An important aspect here is that these dynamic blockage events happen rapidly (e.g., the power degrades fast when the human crosses the communication path), so the communication system often does not have sufficient time to detect the event and react accordingly when the blockage happens. In normal conditions, these dynamic blockage events may last from hundreds of milliseconds up to several seconds, thus violating almost the quality of service (QoS) requirements for almost any traffic category besides the background file transfer [227].

Therefore, the latest studies agree that the human-body blockage must be accounted for in THz channel modeling for use cases and environments that involve human users (or even the pedestrians passing by who are not users). A consensus approach here is to model the human body as a cylinder with a given height and width representing a typical person (e.g., 1.7 cm in height and around 0.4 cm in width). Whenever a certain part of the signal passes through the human body, the corresponding signal is

attenuated by a given number of decibels (usually, no less than 20 dB).

A more advanced option is to model diversity of humans in the environment by defining the cylinder height and width as stochastic variables (e.g., following a normal distribution with a given mean and variance [228]). This approach acknowledges the fact that humans are different from each other but requires greater computational resources (for simulation-based models) as well as leads to more sophisticated analytical expressions (for theoretical models). Finally, the most in-depth approach suggests replacing a first-order cylinder model with more accurate models for different human body parts [229]. This approach improves the accuracy of the resulting models but is exploited relatively rarely due to its notably greater complexity.

Another essential aspect of human-body blockage for indoor/outdoor THz access links is *self-blockage* caused by the body of the human user itself. Here, the most widely adopted approach is to model a fixed separation distance between a THz mobile device and the person holding it. Hence, a certain 2-D or 3-D angle sector gets blocked by the user body, as revealed in [230] and other works on the topic.

### D. Vehicular THz Systems

Following the discussion in Section II, the vehicular environment is one of the promising use cases for THz communications, THz radar, and joint THz communications and sensing solutions. THz hardware components have made significant progress over the recent decade. Still, modern sub-THz (and especially THz) hardware is not sufficiently compact, cost-efficient, and energy-efficient to aim for its successful adoption in next-generation handheld personal devices (such as smartphones, tablets, laptops, or XR glasses). On the contrary, vehicle-mounted systems feature notably less stringent restrictions on their weight (compared to the weight of the vehicle itself), cost, and power budget [231].

However, introducing vehicles to outdoor THz channels leads to several distinct features that require additional efforts in THz channel modeling. First and foremost, the vehicle body itself is a complex obstacle that is neither transparent for THz radiation nor absorbs/reflects it back in every configuration. Specifically, the latest studies show that a promising approach to model the vehicle body in THz channel modeling is by following the layered sandwich-type path. The measurements reported in [232] show that the vehicle body is almost nontransparent at the engine level (up to 0.8 m, on average) while only decreasing the power of the THz signal passing at the windows level (0.8-1.5 m, depending on the vehicle) by a few decibels, as illustrated in Fig. 10. Hence, a two-layer model (vehicle representation with a semi-transparent parallelepiped on top of a nontransparent parallelepiped) is the minimal set needed for THz channel modeling, while

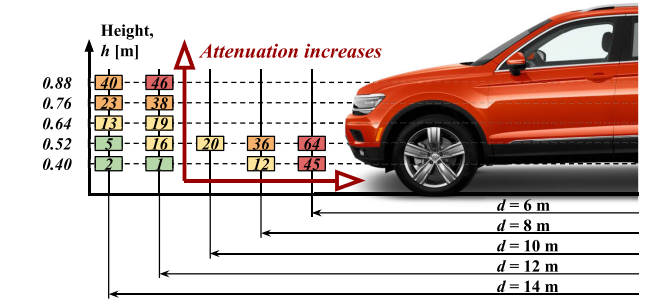


Fig. 10. Nonnegligible under the vehicle propagation in THz vehicular communications at 300 GHz.

additional layers (roof, wheel, and so on) can be added as needed to improve the accuracy further.

The second important distinct feature of vehicular THz setups that should not be neglected in channel modeling is the signal propagation under the vehicle. Depending on the car model, the vehicle clearance (empty space under the vehicle body) may vary from typically 10 to 22 cm. As noticed in many works (from [233] down to [234], among others) and illustrated in 10, this "tunnel" under the vehicle often acts as a waveguide when it comes to vehicular communications (especially, direct vehicle-to-vehicle links), featuring relatively low signal attenuation [232]. Therefore, for more accurate modeling, the two-layer obstacle representation from above should be converted into a three-level model with another 10–20-cm transparent layers added to the bottom.

Finally, the human-body blockage mentioned in the previous section is often modeled with a group of identical (or at least statistically identical) human-body models, as humans are not several times different in size. These models may include nontransparent cylinders of a given height (average human height with zero or nonzero variance) and radius (average human width with zero or nonzero variance) or more sophisticated models of several cylinders/spheres representing different parts of the human body. On the contrary, there are notably different categories of vehicles present on a typical road: from small city cars to trucks, buses, and trams that can be longer than five cars combined. As noted in several studies (including [235] and [236], among others), the presence of such large vehicles may impact a lot the performance of mmWave and THz wireless links and thus must be accounted for in THz channel modeling. One of the feasible approaches here recommended is to develop a set of statistical models for the most common vehicle types (e.g., car, bus, and truck) and then deploy them on-site with a certain proportion following the percentage of those on a typical road.

# E. Summary

In the authors' view, the following are the key takeaways from the latest progress on THz channel modeling.

Key effects	Deployment scenarios					
	Indoor	Outdoor	Vehicular	Vehicular		
Spreading	High	High	High	High		
Absorption	Low	Medium	Medium	High		
Reflection	High	Medium	High	Low		
Scattering	Medium	Low	Medium	Low		
Diffraction	Low	Low	Low	Low		
Blockage	High	Medium	High	Low		
Frample models	[221] [223] [237]_[241]	[29] [31] [198]	[54] [232]	[63] [209]		

Table 2 Importance of Key Propagation Effects in THz Channel Modeling for Different Use Cases

- 1) The THz channel model must be used case-specific and deployment-specific to be sufficiently accurate.
- 2) The characteristics of the THz channel are heavily dependent on the presence/absence of the clear LoS between the TX and the RX; however, concluding that THz links can *only* work within LoS conditions is wrong and simplistic, there are numerous deployment configurations, where NLoS THz links provide sufficient link budget for communication purposes (e.g., through a clear first- or second-order reflection).
- 3) Unlike prior approaches (e.g., 3GPP-driven for 5G-grade systems [242]), it is not always possible to decouple the antenna-related effects from the channel-related effects due to the large size of the THz near=field zone.
- 4) When operating in transparency windows [210] or via relatively narrow THz subbands far from the absorption lines, for indoor setups, molecular absorption effects are of secondary importance compared to blockage, reflection, and scattering from obstacles present in the environment. The situation is the opposite in airborne setups, where absorption plays a nonnegligible role, while the impact of blockage/reflection is often negligible.
- 5) Under-vehicle propagation should not be ignored when modeling THz channels in the presence of cars and other vehicles in the environment.

Concluding two in-depth discussions on THz hardware and THz channel in this section and the previous section, we now proceed with outlining some of the pressing challenges and open research problems in the field given next.

# V. CHALLENGES AND OPEN RESEARCH DIRECTIONS

# A. Next Steps in THz Hardware

1) Toward True THz Ultrabroadband Devices: While the so-called "THz gap" describes the lack of electronics or photonics means to generate and receive THz signals, one of its fundamental causes is the lack of THz electronic, photonic, or plasmonic devices. Therefore, there is a perennial need for electronic or photonic devices that operate efficiently and effectively in the THz frequency bands. In all three approaches, there is a need to increase the

power, frequency of operation, and/or bandwidth. Besides the adoption of non-CMOS or beyond-CMOS technologies, including vertical SiGe HBT devices and InP or GaN devices [19], new materials enter the game. In addition to graphene, other 2-D nanomaterials, such as hexagonal boron nitride (h-BN) or molybdenum disulfide (MoS2), and few-atom-thick heterostructures open the door to new physics and properties that can be leveraged for THz wireless applications [243], [244]. While these technologies will not be ready for 6G, they are likely to be found based on future generations.

2) Circuits and System Architectures: As we discussed in Section III-B, the very small size of individual sub-THz and THz antennas allows their integration in large numbers in very small footprints. However, fitting the front-end electronics and antennas into the small  $\lambda/2$  by  $\lambda/2$  array pitch has become increasingly challenging. One possible solution is to explore ultracompact circuit topologies [245], [246], [247]. Alternatively, one may explore new packaging techniques and new 2-D array architectures. For example, a popular architecture is the array of subarrays [139], [248], in which multiple digital channels control multiple analog chains each. Each analog chain, in turn, might be a fixed array or might incorporate amplitude, phase, or delay controllers.

Alternatively, the adoption of graphene-based plasmonic technologies can lead to the design of fully digital arrays with direct modulation and beamforming weight control per antenna, potentially opening the door to ultramassive MIMO systems [137], [149]. As discussed in Section III-A, submicrometric on-chip plasmonic THz sources and THz modulators together with micrometric plasmonic antennas can lead to extremely compact front ends. Moreover, these front ends leverage the concept of direct RF or antenna modulation, where, as opposed to traditional digital systems in which the in-phase (I) and quadrature (Q) components are generated in baseband digitally before being converted to the analog domain, a few or even a single digital line is utilized to control the amplitude and/or phase of the signal directly at RF [249], [250], [251]. The possibility of replacing large, power-demanding data converters with individual digital lines might lead to new, more compact, and energy-efficient array architectures. While plasmonic technology is relatively at a very early stage, the concepts of direct RF or antenna modulation are also actively explored at mmWave and sub-THz frequencies with CMOS technology.

3) Packaging Technologies: Advanced packaging technologies are foundational to 6G electronics since they enable heterogeneous integration of different components, e.g., antennas, THz front-end circuits, analog baseband circuits, and digital backends, using different process technologies for system-level optimization. The key considerations on packaging technologies include RF performance (loss tangent), pin pitches, fabrication tolerance, thermal handling, thermal expansion, and mass producibility. Widely used in existing RF products, low-temperature cofired ceramic (LTCC) technology offers low-loss tangent and hermetic properties. However, LTCC is limited to thicker substrates, large feature sizes, and smaller panels, which are not compatible with 6G THz electronics that require fine signal pitches and large-scaled array integrations [252]. Liquid crystal polymer (LCP) offers low-loss tangent and low moisture absorption but exhibits a large coefficient of thermal expansion (CTE) and difficulty in creating precise cavities and fine-resolution traces [252]. Recently, there has been an increasing interest in employing glass substrate for 6G sub-THz/THz packaging due to its ultralow-loss tangent, precise metalization, fine signal pitch/density, and low cost. Example D-band radio-onglass and phased-array-on-glass have been demonstrated with excellent performance [253], [254].

### **B.** Next-Generation THz Channel Models

Summarizing the discussion in the previous section on the progress in channel modeling for THz, there are three key challenges ahead toward the design of accurate, flexible, and useful next-generation channel models for THz communications:

1) Near-Field Effects: The major distinct feature of THz communications in comparison to existing 5G-grade mmWave solutions is the nonnegligible near-field zone of THz antennas [255] that lasts for several (tens) of meters. As illustrated in multiple studies (see [256], [257], and [258], among many others), the near-field effect cannot be neglected for THz frequencies, as the received signal gets a notably different structure than with the canonical far-field assumption, Specifically, the antenna gain function in the near field becomes not only angle but also distance-dependent. As discussed further in [152], canonical far-field beamforming can demonstrate up to 7-10-dB difference in the THz near field versus the expected values from existing propagation models. Therefore, accurate and flexible extensions are to be introduced into the nextgeneration THz channel models to account for this important effect.

Another essential feature of near-field THz communications impacting next-generation channel models is the fact that the antenna-related effects cannot be that easily decoupled from the environment-related propagation effects. The key reason here is that the length of the near-field propagation zone (and also the impact on the received signal) heavily depends on the selected antenna configuration [259]. Hence, a commonly used (e.g., in 3GPP TR 38.901 [242]) two-stage approach, where the channel model is first derived assuming omnidirectional propagation and then tailored independently to different antenna configurations, is not directly applicable anymore and has to be modified accordingly [260]. Last but not least, the community also recently started actively exploring alternative wavefronts to complement or replace beamforming for near-field THz communications. These include, among others, beamfocusing, self-healing Bessel beams, and curved-shape Airy beams, all demanding different extensions in next-generation THz channel models [170], [261].

2) Mobile THz Users: Another inherent limitation of existing 5G-grade mmWave and state-of-the-art THz channel models is the fact that the overwhelming majority of them are designed exclusively in stationary conditions, where both communicating nodes do not move during the entire duration of the data exchange. While this is a valid assumption in most cases at lower frequencies, for THz communications with an order of magnitude shorter wavelength, this is not 100% applicable, as even minor changes in the node's location may lead to drastic variations in the received signal. This is especially crucial in the THz near field (as discussed above) and in indoor environments featuring rich multipath. Specifically, a slight change in the node location may change the sim phase/counter phase arrival of multipath components or even lead to a given strong multipath component being added/removed completely from the channel frequency response.

Last but not least, THz communications are envisioned to exploit extremely directional beams. Hence, in combination with large-scale mobility (movements of the user node itself), THz communications are notably affected by microscale (or small-scale) mobility of the mobile device itself (e.g., random displacements and rotations). As illustrated in a few recent studies (including but not limited to [262] and [216]), these small-scale movements (and especially small-scale rotations) may have an even greater impact on the performance of the THz link. Hence, while developing next-generation channel models for stationary THz communications is a valid approach, designing novel types of THz channel models already accounting for possible small- and large-scale mobility of one or both communicating nodes is a much more valuable option and a tempting research direction.

3) Generalized Statistical Channel Models: Developing generalized statistical channel models for THz communications is the third key research direction from today's THz channel models to next-generation approaches suitable for 6G standardization and beyond. Recall that one of our key lessons discussed above is that there is likely no possibility

to develop a "common" THz channel model suitable to all the environments, use cases, and node configurations (e.g., antennas). Therefore, the state-of-the-art vision is that the channel model must be tailored to a specific environment and a specific use case. Indeed, when comparing channel modeling (and especially channel measurement) contributions for sub-THz and THz frequencies, they evolved from general channel models for a wide range of scenarios back in the 2000s and 2010s (e.g., [189]) all the way very in-depth studies on the peculiar effects in a particular corridor or an office environment with this exact layout of furniture [238], [263].

On the one hand, this leads to notably more accurate results. On the other hand, the applicability of these environment-specific THz channel models is ultimately limited to exactly the same environment and the same hardware used for the data exchange. Following the discussion in the two items above, even slight variations introduced into the setup may lead to a notably different picture at the RX. Hence, there is a clear gap here to address when developing next-generation channel models for THz communications—designing a sufficiently general (thus widely applicable) while still sufficiently accurate THz channel model. Some essential research questions here to answer are: 1) what is the required level of detail in the environment that is sufficient for THz channel modeling (e.g., resolution of the obstacles and their materials) and 2) what kind of small- and large-scale mobility can be tolerated without rapid deviations in the channel frequency response.

As of today, one of the promising directions here seems to be following the 3GPP-style approach (e.g., as in TR 38.901 and earlier documents for channel modeling up to 100 GHz), where the model is developed not for a given environment but for a given class of environments (e.g., any outdoor city street or any indoor office building with typical characteristics). Maintaining the balance between accuracy and flexibility is one of the major challenges on the way from existing general THz channel models (not applicable to any given nontrivial scenarios) and existing scenario-specific THz channel models (not applicable to any other specific scenario) toward next-generation THz channel models for various typical classes of use cases and deployment scenarios (e.g., indoor office, outdoor cell, vehicular, and WNoC).

However, the 3GPP modeling approach identifies a large number of "clusters" with each cluster having several multipaths traveling close in both space and time. Empirical observations show that multipaths in the same time cluster can arrive at an RX from different spatial directions and multipaths in a spatial cluster can arrive at distinct times [264]. Moreover, multipaths in outdoor and indoor wireless channels are observed to become sparser when transitioning from mmWave to sub-THz and beyond [265]. With the increased sparsity, deterministic channel modeling using ray-tracing tools, such as NYURay [266], can prove valuable for gaining insight into the propagation

behavior at THz frequencies where accurate maps of the specific environment are available.

The time-cluster spatial-lobe approach models multipath propagation behavior through independent time and spatial clusters and forms the basis for the NYUSIM simulator for channel modeling up to 150 GHz in indoor, outdoor, and factory scenarios [195], [237]. Similarly, tools, such as TeraSim [267], conceived for the simulation of more general applications of THz systems (beyond cellular networks) are also currently being adopted to perform full-stack performance analyses of next-generation cellular networks [268], [269], [270], [271]. Poddar et al. [203, Tables I and II] showcase other popular channel models and simulators for 5G and beyond, many of which will keep evolving to incorporate THz communications in the future.

# C. Building the Physical and Link Layer of THz Networks

The design of the physical and the link layers of THz communication systems needs to capture both today's and the envisioned capabilities of THz radios as well as the peculiarities of the THz channel. In this section, we discuss how different state-of-the-art communication and networking technologies can achieve this goal.

1) Bandwidth Versus Beamwidth—Exploiting the Tradeoff: As discussed in Section II, the applications of THz communications are very diverse, ranging from WNoC to nonterrestrial networks (NTNs). As a result, it is difficult to define typical values for the transmit power, antenna configuration, bandwidth, and, ultimately, achievable bit rate.

The transmit power of a THz radio drastically changes across frequencies. For example, as discussed in Section III-A, the NASA Jet Propulsion Laboratory (JPL) has demonstrated world-record high-power frequency multipliers with nearly 200 mW in the sub-THz range [57]. The same technology at 1 THz exhibits only a few milliwatts. To compensate for the relatively low power and increase the signal strength at the RX, high-gain directional antennas are commonly utilized. Again, as discussed in Section III-B, the small wavelength of THz signals allows for high directivity antennas in a very small footprint. Besides this, is it relevant to note that the ability to close a link at the RX depends not only on the received signal strength but on the total noise at the RX and, ultimately, on the SNR. The noise power itself depends on the technology being used as well as on the total bandwidth. Therefore, there are many cases in which reducing the bandwidth is needed to close the link.

The *bandwidth* of a THz communication system depends on multiple factors, including the hardware capabilities, the channel peculiarities, and the legal limitations. As discussed in Section III, current sub-THz and THz transceiver and antenna architectures can easily support 10 GHz of bandwidth and more, for example, in the

Jornet et al.: Evolution of Applications, Hardware Design, and Channel Modeling: Ready for 6G?

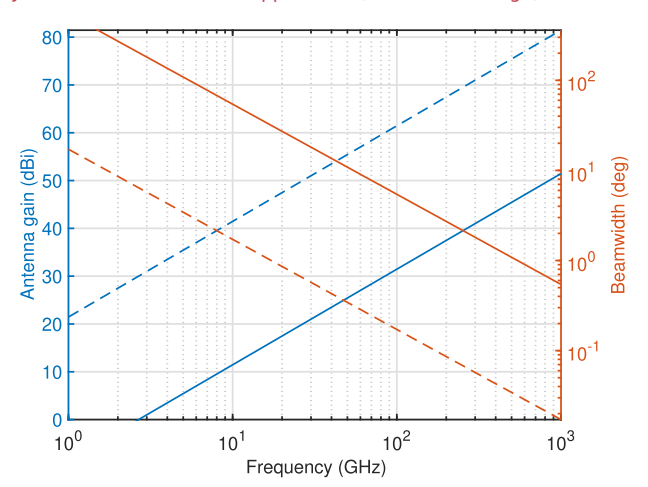


Fig. 11. Antenna gain (blue) and beamwidth (red) as functions of frequency for a fixed antenna footprint of 10 cm $^2$  (solid lines) and 1 m $^2$  (dashed lines).

TeraNova platform at Northeastern University (NU), front ends with 20 GHz of bandwidth at a tunable center frequency between 110 and 170 GHz, 30 GHz between 210 and 240 GHz, and up to 50 GHz between 1 and 1.05 THz [272]. This limit is primarily set by the mixer at the TX and the RX. Regarding the channel, and as presented in Section IV, the available bandwidth is significantly larger. In the sub-THz range, there are only two absorption peaks (at 119 and 183 GHz), theoretically enabling very large transmission windows. Above 300 GHz, there are many more absorption lines, but the separation between them is still of tens and even hundreds of GHz [210]. However, it is first relevant to note that the sub-THz spectrum up to 275 GHz is already allocated to different services, including fixed, mobile, and satellite communications, Earth-Exploration Satellite Service (EESS), and space research [273]. Today, between 100 and 200 GHz, only 12.5 GHz of contiguous bandwidth is allocated to communication services. If sharing with space services is allowed, this value can increase to 32.5 GHz. A similar situation is found between 200 and 275 GHz. An extensive discussion on the coexistence and spectrum sharing issues at frequencies above 100 GHz is given in [274].

To be able to provide quantitative data, next, we focus on indoor WLAN and outdoor cellular applications. First, in Fig. 11, we illustrate the achievable directional gain for a fixed antenna footprint of 10 cm<sup>2</sup> (comparable to that of a current smartphone) as a function of frequency, highlighting the ability to achieve very high gains with a very compact structure. Second, in Fig. 12, we illustrate the tradeoff between antenna beamwidth or directivity and system bandwidth. More specifically, we consider a 30-m LoS link, with a TX delivering 100 mW of output power and 20 dBi of antenna gain and an RX with an NF of 20 dB and an antenna gain ranging from 0 to 40 dBi.

Increasing the bandwidth while maintaining the SNR and, thus, increasing the bit rate requires a major increase in directivity gain, which requires larger radiating structures (though still compact, as per Fig. 11), leading to further near-field effects (with the challenges and opportunities that they bring, as previously discussed), and increased beam management complexity (as we elaborate later in this section). These tradeoffs need to be captured when designing the physical and link layers of THz networks. For example, not all transmissions might need extremely high bit rates, and thus, reducing the bandwidth can automatically relax many other requirements in the system.

Once the feasibility of the link is established, the achievable bit rate with a maximum tolerable bit error rate (BER) depends on the specific modulation technique being used, as we discuss next.

2) Ultra-Broadband Waveform, Modulation, and Coding: The modulation techniques for THz signals have drastically evolved in the last decade. Due to their simplicity, the first THz systems considered only noncoherent modulations, such as ON-OFF keying modulation [275] and, today, this is still one of the two physical layers supported by the only standard for THz systems, the IEEE 802.15.3d [28]. This early approach, together with the very large bandwidth supported by the THz channel, has often resulted in the misleading belief that there is no need for spectrally efficient modulations at THz frequencies. However, as discussed in Section III, current THz transceivers exhibit low transmit power and potentially very high amplitude and phase noise. While antenna gains play a key role in the system performance, the need for spectrally efficient modulations that can maximize the bandwidth utilization and, ultimately, reach terabits per second becomes evident.

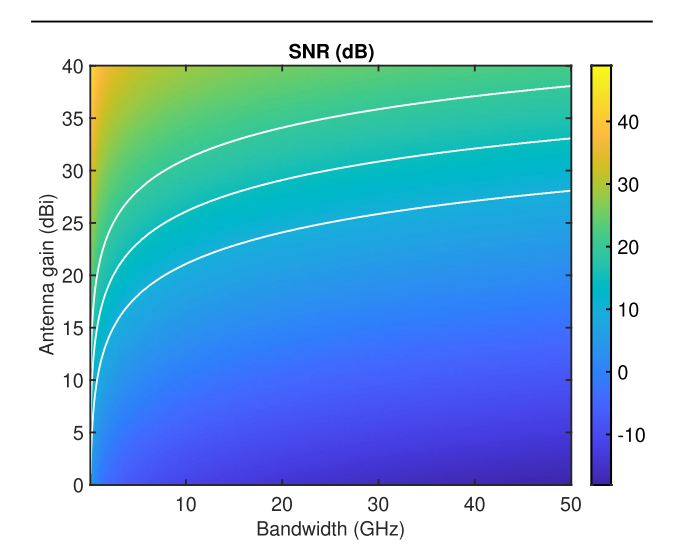


Fig. 12. Required SNR as a function of antenna gain and bandwidth, for a 30-m LoS link at 140 GHz, with a TX with 100 mW of output power and 20 dBi of antenna gain, and an RX with an NF of 20 dB, and an antenna gain ranging from 0 to 40 dBi. The white solid lines indicate the minimum antenna gain to achieve an SNR of at least 10, 15, and 20 dBi.

In this direction, different strategies exist. On the one hand, one can leverage the state-of-the-art modulations in 5G and 5G advanced systems and scale them up in bandwidth. For example, while the use of OFDM might be discouraged due to its high peak-to-average power ratio (PAPR), discrete-Fourier-transform-spread OFDM (DFT-S-OFDM) can be adopted. Similarly, orthogonal timefrequency space (OTFS) modulation could be utilized to compensate for the frequency offsets resulting not only from mobility in some applications but also from the phase noise of THz oscillators. There have been several papers thoroughly comparing these modulations [276], [277], [278]. Most recently, in [279], we have studied the joint impact of PAPR and phase noise on single and multicarrier modulations as well as on ultra-broadband spreadspectrum techniques [280]. Based on newly developed experimentally driven phase noise models at three different sub-THz and THz bands and introducing the concept of PAPR penalty, we have concluded that DFT-S-OFDM offers a fair tradeoff for data rate and BER.

Besides traditional modulations, new waveforms are enabled by the behavior of the THz channel. For example, for very short-range applications, very short pulses, just a few hundred femtoseconds long, can be utilized [189]. The power spectral density of such pulses, commonly used in sensing applications including terahertz (THz) timedomain spectroscopy (THz-TDS), spans a few THz. Their very short duration enables very high symbol rates. For longer communication distances, the molecular absorption broadening effect and the distance-dependent bandwidth discussed in Section IV motivate and enable new modulation techniques that facilitate the multiplexing of users in space. For example, in [281], a modulation scheme that leverages multiple absorption-defined transmission windows and dynamically allocates a different number of subcarriers per window based on the users' distance is presented. In [282], a hierarchical-bandwidth modulation scheme that multiplexes in a single stream data with different modulation orders and symbol durations is proposed as a way to transform molecular absorption into an ally to spatially multiplex users within the same transmission beam.

Finally, in terms of error control coding, much less has been done. For the time being, the only discussions on error control are focused on the nanoscale applications of the THz band and advocate for the use of low-weight codes, i.e., codewords with more binary zeros than ones, as a way to simultaneously minimize molecular absorption noise and multiuser interference [283], [284], [285]. New error control strategies tailored to the imperfections of THz hardware, including device-induced frequency selectivity and large amplitude and phase noises, and the behavior of the channel, such as the frequency selectivity of molecular absorption, are needed all while keeping an eye toward low computational complexity, so to meet the latency requirements of 6G.

3) Channel Estimation and Beam Management: As just discussed, the high gain and narrow beamwidths are crucial in enabling THz communications. To implement mobile sub-THz and THz wireless communications, it is necessary to implement beamforming to steer the radiated signal or to control the direction of reception while communicating with multiple transceivers [286]. Hybrid beamforming architectures that use digital beamforming at the baseband with analog beamforming at the RF are already used in today's mmWave 5G cellphones and are anticipated to be widely utilized for THz transceivers. Digital beamforming facilitates spatial multiplexing gains, while analog beamforming—through phase shifters at the RF—offers directionality gains from the radiating antenna [287]. As per the discussion in Section V-A, if fully digital antenna arrays become available, both multiplexing and beamforming gains can be combined and digitally implemented.

Channel estimation is pivotal to provide the proper channel state in order for the analog and digital beamforming vectors to be adapted for proper pointing directions to maximize link gain while minimizing interference [286] for THz communication systems. Achieving optimal beamforming relies on perfect prior knowledge of the channel matrix and its singular value decomposition. Omnidirectional pilot signals are not practical in highly directional THz channels due to severe path loss and blockage, so beamforming must learn the channel to estimate the channel response and determine the best antenna beamform weightings for the current channel state.

One approach for channel estimation can involve using exhaustive beam training to explore the entire spatial search space, aiming to establish a beamforming link between transceivers. Careful codebook design can help expedite the search to identify the most suitable narrowbeam pair with the highest SNR [248]. As an example, IEEE 802.11ad uses a one-side exhaustive search protocol [248], [286] whereby a user performs an exhaustive search across all beams in the codebook, while the AP transmits with an omnidirectional beam. Moreover, to reduce the training overhead and spatial search space associated with exhaustive beam training that searches over every AoD/AoA pair, adaptive channel estimation algorithms utilizing codebooks with multiple spatial resolutions can accelerate the search process. In addition, compressed sensing-based beamforming methods can take advantage of the sparsity of multipath in the channel to obtain channel state information [288]. Deep learningbased methods leveraging convolutional neural networks for channel estimation have also demonstrated promising results, making them potential candidates for accurate THz channel estimation [289]. Finally, less conventional antenna designs, such as leaky wave antennas, and new array operations, such as the joint phase-time array and the frequency-modulated array (FMA), which all exhibit unique frequency-AoD relationships, can be utilized to expedite neighbor discovery [290], [291], [292].

Jornet et al.: Evolution of Applications, Hardware Design, and Channel Modeling: Ready for 6G?

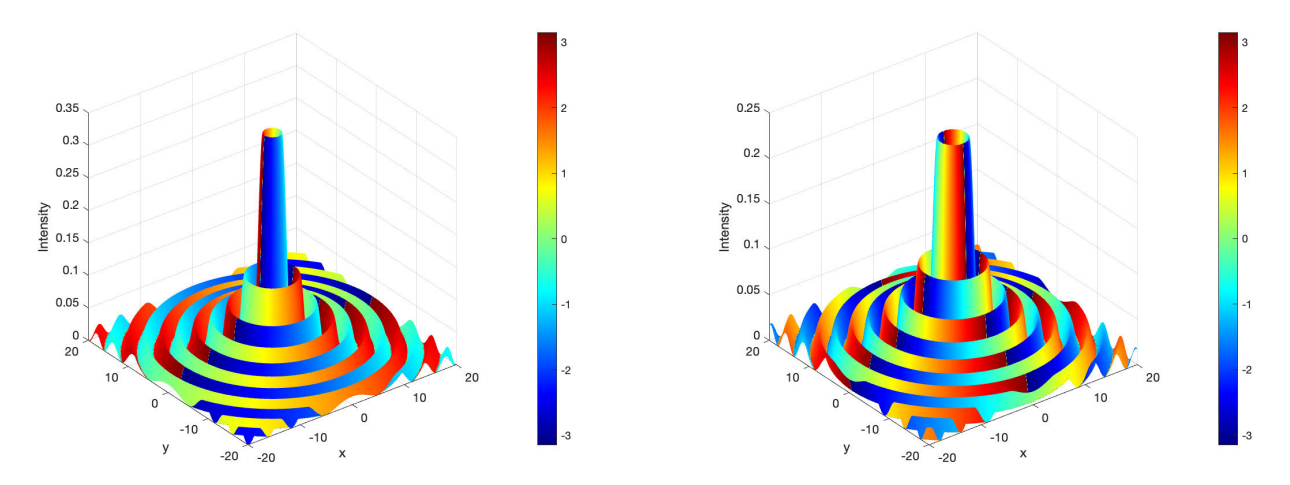


Fig. 13. Intensity (height) and phase (color) profile of two different OAM modes (helical Mode 1 on the left and helical Mode 2 on the right). The two modes are orthogonal and define an orthogonal basis that can be used for information modulation or multiplexing.

4) Ultramassive/XL-MIMO, Cell-Free MIMO, and Orbital Angular Momentum: Up to this point, it has been mostly considered that the very large antenna arrays at THz frequencies will be primarily leveraged to generate highly directional narrow beams and, thus, increase the SNR of a single path and, correspondingly, the modulation order it can support. However, there are scenarios where higher gains can be achieved by exploiting spatial multiplexing. Many are the works that discuss theoretical solutions for THz massive, ultramassive, and XL-MIMO (see [149], [248], [293], [294], and [295], and only recently, experimental works have been conducted. In [240], we have recently experimentally demonstrated that there exists enough diversity in common indoor scenarios to support MIMO systems with channels over geometrically different paths. Building on this result and the aforementioned advantages of DFT-S-OFDM, we have designed and built a functioning MIMO system over 10 GHz of bandwidth [296].

For the cases in which the channel does not naturally support orthogonal paths, diversity can be achieved using orbital angular momentum (OAM). A beam that is said to have OAM manifests a spiral phase in the transverse direction, resulting in a helical wavefront and a phase singularity (a zero-intensity vortex) in the center. Overlapping beams that follow helical modes define an orthogonal basis (see Fig. 13). This can be leveraged in different ways. Different streams can be sent along different OAM modes, each one with its own amplitude and/or phase modulation, or one stream can be sent by encoding different symbols in different OAM modes.

Finally, it is worth mentioning that very little has been studied when it comes to distributed or cell-free massive MIMO [297] at THz frequencies. For example, in [298], THz communications are utilized to interconnect the distributed APs that implement cell-free massive MIMO, but not as the access technology itself. The main reason for this would be the extremely precise synchronization that

would needed to enable any form of distributed MIMO or wavefront engineering at THz frequencies.

5) Network-Level Integration of Advanced Physical Layer Technologies: Up to this point, we have discussed the role that different advanced physical layer solutions might play at THz frequencies. However, there is one last aspect that we would like to highlight: the use of extremely narrow beams, the coordination among users in distributed or cellfree massive MIMO or the orchestration of all the network resources (including the RISs discussed in Section III-B), can introduce significant delays, impacting the latency, the throughput, and, above all, the users' QoS or quality of experience (QoE). For example, if finding the optimal NLoS path between two users through a RIS requires even a few milliseconds, one should consider directly switching, even if temporarily, to a lower unobstructed frequency band (e.g., sub-6 GHz) if multiband radios are available [299]. At this stage, while many optimization frameworks have been developed at the physical layer, few solutions consider the actual end-to-end delay, including the latency introduced by the control channel, which is ultimately what the user experiences. Now, it is time to go up in the protocol stack to ensure the success and broad adoption of the THz band for communications [269].

### VI. CONCLUSION

This article summarizes the latest progress in the field of THz communications and sensing, specifically focusing on the hardware aspects (such as closing the "THz gap") and the latest advancements in THz channel modeling. Our main conclusion is that over the last two decades, THz communications evolved rapidly from "futuristic vision" to "forthcoming reality." Wireless connectivity and sensing above 100 GHz are now of great interest already within the 6G timeline (2030 onward, only five years from now). While we will likely not see the full power of THz radios in the first 6G releases, the principal step toward adopting

the THz spectrum for commercial radio systems and networks has clearly been made. Still, as summarized above, there are multiple research and engineering challenges to be addressed toward enabling reliable and efficient THz wireless systems and networks.

#### REFERENCES

- T. S. Rappaport et al., "Millimeter wave mobile communications for 5G cellular: It will work!" IEEE Access, vol. 1, pp. 335–349, 2013.
- R. Vannithamby and A. Soong, 5G Verticals: Customizing Applications, Technologies and Deployment Techniques. Hoboken, NJ, USA: Wiley, 2020.
- [3] T. S. Rappaport et al., "Wireless communications and applications above 100 GHz: Opportunities and challenges for 6G and beyond," *IEEE Access*, vol. 7, pp. 78729–78757, 2019.
- [4] I. F. Akyildiz, A. Kak, and S. Nie, "6G and beyond: The future of wireless communications systems," *IEEE Access*, vol. 8, pp. 133995–134030, 2020.
- [5] M. Giordani, M. Polese, M. Mezzavilla, S. Rangan, and M. Zorzi, "Toward 6G networks: Use cases and technologies," *IEEE Commun. Mag.*, vol. 58, no. 3, pp. 55–61, Mar. 2020.
- [6] W. Saad, M. Bennis, and M. Chen, "A vision of 6G wireless systems: Applications, trends, technologies, and open research problems," *IEEE Netw.*, vol. 34, no. 3, pp. 134–142, May/Jun. 2019.
- [7] H. Tataria, M. Shafi, A. F. Molisch, M. Dohler, H. Sjöland, and F. Tufvesson, "6G wireless systems: Vision, requirements, challenges, insights, and opportunities," *Proc. IEEE*, vol. 109, no. 7, pp. 1166–1199, Jul. 2021.
- [8] I. F. Akyildiz, J. M. Jornet, and C. Han, "Terahertz band: Next frontier for wireless communications," *Phys. Commun.*, vol. 12, pp. 16–32, Sep. 2014.
- [9] Z. Chen et al., "A survey on terahertz communications," *China Commun.*, vol. 16, no. 2, pp. 1–35, Feb. 2019.
- [10] Y. Xing, O. Kanhere, S. Ju, and T. S. Rappaport, "Indoor wireless channel properties at millimeter wave and sub-terahertz frequencies," in *Proc. IEEE Global Commun. Conf. (GLOBECOM)*, Dec. 2019, pp. 1–6.
- [11] H. Sarieddeen, N. Saeed, T. Y. Al-Naffouri, and M.-S. Alouini, "Next generation terahertz communications: A rendezvous of sensing, imaging, and localization," *IEEE Commun. Mag.*, vol. 58, no. 5, pp. 69–75, May 2020.
- [12] Y. Xing and T. S. Rappaport, "Millimeter wave and terahertz urban microcell propagation measurements and models," *IEEE Commun. Lett.*, vol. 25, no. 12, pp. 3755–3759, Dec. 2021.
- [13] H.-J. Song and N. Lee, "Terahertz communications: Challenges in the next decade," *IEEE Trans. THz Sci. Technol.*, vol. 12, no. 2, pp. 105–117, Mar. 2022.
- [14] S. Ju and T. S. Rappaport, "Sub-terahertz spatial statistical MIMO channel model for urban microcells at 142 GHz," in *Proc. IEEE Global* Commun. Conf. (GLOBECOM), Dec. 2021, pp. 1–6.
- [15] C. Chaccour, M. N. Soorki, W. Saad, M. Bennis, P. Popovski, and M. Debbah, "Seven defining features of terahertz (THz) wireless systems: A fellowship of communication and sensing," *IEEE Commun. Surveys Tuts.*, vol. 24, no. 2, pp. 967–993, 2nd Quart., 2022.
- [16] I. F. Akyildiz, C. Han, Z. Hu, S. Nie, and J. M. Jornet, "Terahertz band communication: An old problem revisited and research directions for the next decade," *IEEE Trans. Commun.*, vol. 70, no. 6, pp. 4250–4285, Jun. 2022.
- [17] T. S. Rappaport, K. A. Remley, C. Gentile, A. F. Molisch, and A. Zajić, Radio Propagation Measurements and Channel Modeling: Best Practices for Millimeter-Wave and Sub-Terahertz Frequencies. Cambridge, U.K.: Cambridge Univ. Press, 2022.
- [18] A. Shafie, N. Yang, C. Han, J. M. Jornet, M. Juntti, and T. Kurner, "Terahertz communications for 6G and beyond wireless networks: Challenges, key advancements, and opportunities," *IEEE Netw.*, vol. 37, no. 3, pp. 162–169, Sep. 2022.
- [19] T. Kurner, D. Mittleman, and T. Nagatsuma, THz

- Communications: Paving the Way Towards Wireless Tbps. Switzerland: Springer, 2022.
- [20] S. Abadal, M. Iannazzo, M. Nemirovsky, A. Cabellos-Aparicio, H. Lee, and E. Alarcón, "On the area and energy scalability of wireless network-on-chip: A model-based benchmarked design space exploration," *IEEE/ACM Trans. Netw.*, vol. 23, no. 5, pp. 1501–1513, Oct. 2015.
- [21] R. Guirado, A. Rahimi, G. Karunaratne, E. Alarcón, A. Sebastian, and S. Abadal, "Wireless on-chip communications for scalable in-memory hyperdimensional computing," in *Proc. Int. Joint Conf. Neural Netw. (IJCNN)*, Jul. 2022, pp. 1–8.
- [22] S. Sun, T. S. Rappaport, R. W. Heath Jr., A. Nix, and S. Rangan, "MIMO for millimeter-wave wireless communications: Beamforming, spatial multiplexing, or both?" *IEEE Commun. Mag.*, vol. 52, no. 12, pp. 110–121, Dec. 2014.
- [23] V. Petrov et al., "Terahertz band intra-chip communications: Can wireless links scale modern x86 CPUs?" *IEEE Access*, vol. 5, pp. 6095–6109, 2017.
- [24] V. Petrov, J. Kokkoniemi, D. Moltchanov, J. Lehtomäki, and Y. Koucheryavy, "Enabling simultaneous cooling and data transmission in the terahertz band for board-to-board communications," *Phys. Commun.*, vol. 22, pp. 9–18, Mar. 2017.
- [25] R. H. Katz, "Tech titans building boom," *IEEE Spectr.*, vol. 46, no. 2, pp. 40–54, Feb. 2009.
- [26] C.-L. Cheng, S. Sangodoyin, and A. Zajić, "THz cluster-based modeling and propagation characterization in a data center environment," *IEEE Access*, vol. 8, pp. 56544–56558, 2020.
- [27] J. M. Eckhardt, C. Herold, B. Friebel, N. Dreyer, and T. Kürner, "Realistic interference simulations in a data center offering wireless communication at low terahertz frequencies," in Proc. Int. Symp. Antennas Propag. (ISAP), 2021, pp. 1–2.
- [28] V. Petrov, T. Kurner, and I. Hosako, "IEEE 802.15.3d: First standardization efforts for sub-Terahertz band communications toward 6G," *IEEE Commun. Mag.*, vol. 58, no. 11, pp. 28–33, Nov. 2020.
- [29] Y. Amarasinghe, W. Zhang, R. Zhang, D. M. Mittleman, and J. Ma, "Scattering of terahertz waves by snow," J. Infr., Millim., THz Waves, vol. 41, no. 2, pp. 215–224, Feb. 2020.
- [30] P. Sen et al., "Terahertz communications can work in rain and snow: Impact of adverse weather conditions on channels at 140 GHz," in Proc. 6th ACM Workshop Millimeter-Wave THz Netw. Sens. Syst., 2022, pp. 13–18.
- [31] P. Li et al., "Performance degradation of terahertz channels in emulated rain," Nano Commun. Netw., vol. 35, Mar. 2023, Art. no. 100431.
- [32] I. F. Akyildiz and J. M. Jornet, "Electromagnetic wireless nanosensor networks," *Nano Commun. Netw.*, vol. 1, no. 1, pp. 3–19, Mar. 2010.
- [33] J. M. Jornet and A. Sangwan, "Nanonetworking in the terahertz band and beyond," *IEEE Nanotechnol. Mag.*, vol. 17, no. 3, pp. 21–31, Jun. 2023.
- [34] I. F. Akyildiz and J. M. Jornet, "The Internet of Nano-Things," *IEEE Wireless Commun.*, vol. 17, no. 6, pp. 58–63, Dec. 2010.
- [35] K. Yang et al., "A comprehensive survey on hybrid communication in context of molecular communication and terahertz communication for body-centric nanonetworks," *IEEE Trans. Mol., Biol. Multi-Scale Commun.*, vol. 6, no. 2, pp. 107–133, Nov. 2020.
- [36] D. M. Mittleman, "Twenty years of terahertz imaging," *Opt. Exp.*, vol. 26, no. 8, pp. 9417–9431, Apr. 2018.
- [37] G. Valušis, A. Lisauskas, H. Yuan, W. Knap, and H. G. Roskos, "Roadmap of terahertz imaging 2021," Sensors, vol. 21, no. 12, p. 4092,

- Jun. 2021.
- [38] I. V. A. K. Reddy, S. Elmaadawy, E. P. Furlani, and J. M. Jornet, "Photothermal effects of terahertz-band and optical electromagnetic radiation on human tissues," Sci. Rep., vol. 13, no. 1, p. 14643, Sep. 2023.
- [39] T. Rappaport, R. Heath, R. Daniels, and J. Murdock, Millimeter Wave Wireless Communications. Upper Saddle River, NJ, USA: Prentice-Hall, 2015.
- [40] H.-J. Song, H. Hamada, and M. Yaita, "Prototype of KIOSK data downloading system at 300 GHz: Design, technical feasibility, and results," *IEEE Commun. Mag.*, vol. 56, no. 6, pp. 130–136, Jun. 2018.
- [41] V. Petrov, D. Moltchanov, and Y. Koucheryavy, "Applicability assessment of terahertz information showers for next-generation wireless networks," in *Proc. IEEE Int. Conf. Commun. (ICC)*, May 2016, pp. 1–7.
- [42] V. Petrov, J. Kokkoniemi, D. Moltchanov, J. Lehtomaki, Y. Koucheryavy, and M. Juntti, "Last meter indoor terahertz wireless access: Performance insights and implementation roadmap," *IEEE Commun. Mag.*, vol. 56, no. 6, pp. 158–165, Jun. 2018.
- [43] M. Gapeyenko, V. Petrov, S. Paris, A. Marcano, and K. I. Pedersen, "Standardization of extended reality (XR) over 5G and 5G-advanced 3GPP new radio," *IEEE Netw.*, vol. 37, no. 4, pp. 22–28, Jul. 2023.
- [44] J. M. Jornet et al., "Optogenomic interfaces: Bridging biological networks with the electronic digital world," *Proc. IEEE*, vol. 107, no. 7, pp. 1387–1401. Jul. 2019.
- [45] P. Sen, J. V. Siles, N. Thawdar, and J. M. Jornet, "Multi-kilometre and multi-gigabit-per-second sub-terahertz communications for wireless backhaul applications," Nat. Electron., vol. 6, no. 2, pp. 164–175, 2023.
- [46] A. A. Boulogeorgos, J. M. Jornet, and A. Alexiou, "Directional terahertz communication systems for 6G: Fact check," *IEEE Veh. Technol. Mag.*, vol. 16, no. 4, pp. 68–77, Dec. 2021.
- [47] D. Morales and J. M. Jornet, "ADAPT: An adaptive directional antenna protocol for medium access control in terahertz communication networks," Ad Hoc Netw., vol. 119, Aug. 2021, Art. no. 102540.
- [48] Q. Xia and J. M. Jornet, "Expedited neighbor discovery in directional terahertz communication networks enhanced by antenna side-lobe information," *IEEE Trans. Veh. Technol.*, vol. 68, no. 8, pp. 7804–7814, Aug. 2019.
- [49] Q. Xia and J. M. Jornet, "Routing protocol design for directional and buffer-limited terahertz communication networks," in Proc. IEEE Int. Conf. Commun. (ICC), Jun. 2020, pp. 1–7.
- [50] F. Norouzian, E. G. Hoare, E. Marchetti, M. Cherniakov, and M. Gashinova, "Next generation, low-THz automotive radar—The potential for frequencies above 100 GHz," in Proc. 20th Int. Radar Symp. (IRS), Jun. 2019, pp. 1–7.
- [51] S. Jiang, G. Charan, and A. Alkhateeb, "LiDAR aided future beam prediction in real-world millimeter wave V2I communications," *IEEE Wireless Commun. Lett.*, vol. 12, no. 2, pp. 212–216, Feb. 2023.
- [52] A. Vasilyev, N. Satyan, G. Rakuljic, and A. Yariv, "Terahertz chirp generation using frequency stitched VCSELs for increased LiDAR resolution," in Proc. Conf. Lasers Electro-Opt. (CLEO), May 2012, pp. 1–2.
- [53] O. Kanhere, A. Chopra, A. Thornburg, T. S. Rappaport, and S. S. Ghassemzadeh, "Performance impact analysis of beam switching in millimeter wave vehicular communications," in Proc. IEEE 93rd Veh. Technol. Conf. (VTC-Spring),

- Apr. 2021, pp. 1-7.
- [54] K. Guan et al., "Measurement, simulation, and characterization of train-to-infrastructure inside-station channel at the terahertz band," *IEEE Trans. THz Sci. Technol.*, vol. 9, no. 3, pp. 291–306, May 2019.
- [55] V. Petrov et al., "On unified vehicular communications and radar sensing in millimeter-wave and low terahertz bands," *IEEE Wireless Commun.*, vol. 26, no. 3, pp. 146–153, Jun. 2019.
- [56] W. Xia, V. Semkin, M. Mezzavilla, G. Loianno, and S. Rangan, "Multi-array designs for mmWave and sub-THz communication to UAVs," in *Proc. IEEE* 21st Int. Workshop Signal Process. Adv. Wireless Commun. (SPAWC), May 2020, pp. 1–5.
- [57] J. V. Siles, K. B. Cooper, C. Lee, R. H. Lin, G. Chattopadhyay, and I. Mehdi, "A new generation of room-temperature frequency-multiplied sources with up to 10× higher output power in the 160-GHz–1.6-THz range," *IEEE Trans. Terahertz Sci. Technol.*, vol. 8, no. 6, pp. 596–604, Nov. 2018.
- [58] P. H. Siegel, "THz instruments for space," IEEE Trans. Antennas Propag., vol. 55, no. 11, pp. 2957–2965, Nov. 2007.
- [59] H. Wang et al. (2000). Power Amplifiers Performance Survey 2000-present. Accessed: Dec. 31, 2023. [Online]. Available: https://ideas.ethz.ch/Surveys/pa-survey.html
- [60] A. J. Alqaraghuli, H. Abdellatif, and J. M. Jornet, "Performance analysis of a dual terahertz/Ka band communication system for satellite mega-constellations," in Proc. IEEE 22nd Int. Symp. World Wireless, Mobile Multimedia Netw. (WoWMoM), Jun. 2021, pp. 316–322.
- [61] Z. Yang, W. Gao, and C. Han, "A universal attenuation model of terahertz wave in space-air-ground channel medium," *IEEE Open J. Commun. Soc.*, vol. 5, pp. 2333–2342, 2024.
- [62] A. J. Alqaraghuli, J. V. Siles, and J. M. Jornet, "The road to high data rates in space: Terahertz vs. optical wireless communication," *IEEE Aerosp. Electron. Syst. Mag.*, vol. 38, no. 6, pp. 4–13, Jun. 2023.
- [63] W. Gao, C. Han, and Z. Chen, "Attenuation and loss of spatial coherence modeling for atmospheric turbulence in terahertz UAV MIMO channels," *IEEE Trans. Wireless Commun.*, early access, Apr. 9, 2024, doi: 10.1109/TWC.2024.3384036.
- [64] S. A. Torrens, V. Petrov, and J. M. Jornet, "Modeling interference from millimeter wave and terahertz bands cross-links in low earth orbit satellite networks for 6G and beyond," *IEEE J. Sel. Areas Commun.*, vol. 42, no. 5, pp. 1371–1386, May 2024.
- [65] Z. Popovic and E. N. Grossman, "THz metrology and instrumentation," *IEEE Trans. THz Sci. Technol.*, vol. 1, no. 1, pp. 133–144, Sep. 2011.
- [66] D. Shakya et al., "Exploring millimeter-wave and terahertz circuits and systems with a novel multiuser measurement facility: Multiuser terahertz measurement facility (THz Lab)," *IEEE Microw. Mag.*, vol. 25, no. 2, pp. 68–79, Jan. 2023.
- [67] D. M. Pozar, Microwave Engineering. Hoboken, NJ, USA: Wiley, 2011.
- [68] H. Bameri and O. Momeni, "A high-gain mm-wave amplifier design: An analytical approach to power gain boosting," *IEEE J. Solid-State Circuits*, vol. 52, no. 2, pp. 357–370, Feb. 2017.
- [69] D.-W. Park, D. R. Utomo, B. H. Lam, S.-G. Lee, and J.-P. Hong, "A 230–260-GHz wideband and high-gain amplifier in 65-nm CMOS based on dual-peak G<sub>max</sub>-core," *IEEE J. Solid-State* Circuits, vol. 54, no. 6, pp. 1613–1623, Jun. 2019.
- [70] X. Tang, J. Nguyen, G. Mangraviti, Z. Zong, and P. Wambacq, "A 140 GHz T/R front-end module in 22 nm FD-SOI CMOS," in Proc. IEEE Radio Freq. Integr. Circuits Symp. (RFIC), Jun. 2021, pp. 35–38.
- [71] G. De Filippi, L. Piotto, A. Bilato, and A. Mazzanti, "A SiGe BiCMOS D-band LNA with gain boosted by local feedback in common-emitter transistors," in Proc. IEEE Radio Freq. Integr. Circuits

- Symp. (RFIC), Jun. 2023, pp. 133–136.

  [72] E. Johnson, "Physical limitations on frequency and power parameters of transistors." in Proc. IRF
- power parameters of transistors," in *Proc. IRE*Int. Conv. Rec., Jan. 1966, pp. 27–34.

  [73] H. Wang, Y. Liu, and N. S. Mannem. (2023).
- [/3] H. Wang, Y. Liu, and N. S. Mannem. (2023). Phased Array Survey 2010-Present. Accessed: Dec. 12, 2023. [Online]. Available: https://ideas.ethz.ch/Surveys/phased-arraysurvey.html
- [74] J. Kim, C.-G. Choi, K. Lee, K. Kim, S.-U. Choi, and H.-J. Song, "A broadband D-band dual-peak gmax-core amplifier with a T-shaped embedding network in CMOS," *IEEE Trans. Microw. Theory Techn.*, vol. 71, no. 5, pp. 1866–1876, May 2023.
- [75] S. Li and G. M. Rebeiz, "High efficiency D-band multiway power combined amplifiers with 17.5–19-dBm psat and 14.2–12.1% peak PAE in 45-nm CMOS RFSOI," *IEEE J. Solid-State Circuits*, vol. 57, no. 5, pp. 1332–1343, May 2022.
- [76] P. Hetterle, A. Engelmann, F. Probst, R. Weigel, and M. Dietz, "Design of a low voltage D-band LNA in 22 nm FDSOI," in Proc. 17th Eur. Microw. Integr. Circuits Conf. (EuMIC), Sep. 2022, pp. 252–255.
- [77] C. J. Lee, H. Nam, D. Kim, S.-K. Kim, and D. Y. Lee, "A D-band variable gain low noise amplifier in a 28-nm CMOS process for 6G wireless communications," *IEEE Trans. Circuits Syst. II*, Exp. Briefs, vol. 71, no. 1, pp. 131–135, Jan. 2024.
- [78] H. Lee, B. Yun, H. Jeon, W. Keum, S.-G. Lee, and K.-S. Choi, "A *D*-band wideband low-noise amplifier adopting pseudo-simultaneous noise and input matched dual-peak G<sub>max</sub>-core," *IEEE Trans. Microw. Theory Techn.*, vol. 72, no. 5, pp. 3260–3273, May 2024.
- [79] B. Yun, D.-W. Park, H. U. Mahmood, D. Kim, and S.-G. Lee, "A D-band high-gain and low-power LNA in 65-nm CMOS by adopting simultaneous noise- and input-matched gmax-core," *IEEE Trans. Microw. Theory Techn.*, vol. 69, no. 5, pp. 2519–2530, May 2021.
- [80] S. Callender et al., "A fully integrated 160-Gb/s D-band transmitter achieving 1.1-pJ/b efficiency in 22-nm FinFET," *IEEE J. Solid-State Circuits*, vol. 57, no. 12, pp. 3582–3598, Dec. 2022.
- [81] A. Agrawal et al., "A 128-Gb/s D-band receiver with integrated PLL and ADC achieving 1.95-pJ/b efficiency in 22-nm FinFET," *IEEE J. Solid-State Circuits*, vol. 58, no. 12, pp. 3364–3379, Dec. 2023.
- [82] J.-H. Park, D.-Y. Yang, K.-J. Choi, and B.-S. Kim, "D-band × 8 frequency multiplier using complementary differential frequency doubler," *IEEE Microw. Wireless Technol. Lett.*, vol. 33, no. 3, pp. 311–314, Mar. 2023.
- [83] M. Möck, I. K. Aksoyak, and A. Ç. Ulusoy, "A high-efficiency D-band frequency doubler in 22-nm FDSOI CMOS," in Proc. 17th Eur. Microw. Integr. Circuits Conf. (EuMIC), Sep. 2022, pp. 272–275.
- [84] S. Park et al., "A D-band low-power and high-efficiency frequency multiply-by-9 FMCW radar transmitter in 28-nm CMOS," *IEEE J. Solid-State Circuits*, vol. 57, no. 7, pp. 2114–2129, Jul. 2022.
- [85] E. Chou et al., "A low-power and energy-efficient D-band CMOS four-channel receiver with integrated LO generation for digital beamforming arrays," in Proc. IEEE 48th Eur. Solid State Circuits Conf. (ESSCIRC), Sep. 2022, pp. 489–492.
- [86] A. Hamani et al., "A 108-Gb/s 64-QAM CMOS D-band RX with integrated LO generation," *IEEE Solid-State Circuits Lett.*, vol. 3, pp. 202–205, 2020.
- [87] S. Li, Z. Zhang, B. Rupakula, and G. M. Rebeiz, "An eight-element 140-GHz wafer-scale IF beamforming phased-array receiver with 64-QAM operation in CMOS RFSOI," *IEEE J. Solid-State Circuits*, vol. 57, no. 2, pp. 385–399, Feb. 2022.
- 88] C. Wang and G. Rebeiz, "A 2-channel 136–156 GHz dual down-conversion I/Q receiver with 30 dB gain and 9.5 dB NF using CMOS 22 nm FDSOI," in Proc. IEEE Radio Freq. Integr. Circuits Symp. (RFIC), Jun. 2021, pp. 219–222.

- [89] A. Hamani et al., "A 84.48-Gb/s 64-QAM CMOS D-band channel-bonding Tx front-end with integrated multi-LO frequency generation," *IEEE Solid-State Circuits Lett.*, vol. 3, pp. 346–349, 2020.
- [90] A. Hamani et al., "A D-band multichannel TX system-in-package achieving 84.48 Gb/s with 64-QAM based on 45-nm CMOS and low-cost PCB technology," *IEEE Trans. Microw. Theory Techn.*, vol. 70, no. 7, pp. 3385–3395, Jul. 2022.
- 91] S. Li, Z. Zhang, and G. M. Rebeiz, "An eight-element 136–147 GHz wafer-scale phased-array transmitter with 32 dBm peak EIRP and >16 gbps 16 QAM and 64 QAM operation," *IEEE J. Solid-State Circuits*, vol. 57, no. 6, pp. 1635–1648, Jun. 2022.
- [92] J. L. González-Jiménez et al., "A D-band transmitter achieving 57.6-Gb/s and 30-dBm EIRP based on channel-aggregation 45-nm ICs and a low-profile flat lens antenna," *IEEE Trans. Microw. Theory Techn.*, vol. 72, no. 1, pp. 836–850, Jan. 2024.
- [93] K. Sengupta, T. Nagatsuma, and D. M. Mittleman, "Terahertz integrated electronic and hybrid electronic-photonic systems," *Nature Electron.*, vol. 1, no. 12, pp. 622–635, Dec. 2018.
- [94] W. R. Deal, K. Leong, A. Zamora, B. Gorospe, K. Nguyen, and X. B. Mei, "A 660 GHz up-converter for THz communications," in Proc. IEEE Compound Semiconductor Integr. Circuit Symp. (CSICS), Oct. 2017, pp. 1–4.
- [95] E. D. Cohen, "The MIMIC program—A retrospective," *IEEE Microw. Mag.*, vol. 13, no. 4, pp. 77–88, May 2012.
- [96] J. J. Sowers et al., "A 36 W, V-band, solid state source," in *IEEE MTT-S Int. Microw. Symp. Dig.*, Jun. 1999, pp. 235–238.
- [97] K. Shinohara et al., "Scaling of GaN HEMTs and Schottky diodes for submillimeter-wave MMIC applications," *IEEE Trans. Electron Devices*, vol. 60, no. 10, pp. 2982–2996, Oct. 2013.
- [98] M. Božanić and S. Sinha, "Emerging transistor technologies capable of terahertz amplification: A way to re-engineer terahertz radar sensors," Sensors, vol. 19, no. 11, p. 2454, May 2019.
- [99] K. Felch et al., "Operating experience on six 110 GHz, 1 MW gyrotrons for ECH applications," Nucl. Fusion, vol. 48, no. 5, May 2008, Art. no. 054008.
- [100] S. S. M. Roberg and S. Chen, "Qorvo millimeter wave GaN MMIC processes, circuits & integration technology," in *Proc. Workshop, mm-Wave GaN MMICs*, 2022, pp. 570–572.
- [101] D. Denninghoff, "High-efficiency GaN MMIC technologies for W-band applications and beyond," in Proc. Workshop, mm-Wave GaN MMICs, 2022.
- [102] F. Thome, E. Ture, P. Bruckner, R. Quay, and O. Ambacher, "W-band SPDT switches in planar and tri-gate 100-nm gate-length GaN-HEMT technology," in Proc. 11th German Microw. Conf. (GebMiC), Mar. 2018, pp. 331–334.
- [103] M. Rocchi, "100,60 and 40 nm GaN/Si power amplifiers to complement Si solutions for 5G and 6G applications," in Proc. Workshop, mm-Wave GaN MMICs, 2022.
- [104] K. Brown et al., "7kW GaN W-band transmitter," in IEEE MTT-S Int. Microw. Symp. Dig., May 2016, pp. 1–3.
- [105] R. Weber et al., "A beyond 110 GHz GaN cascode low-noise amplifier with 20.3 dBm output power," in *IEEE MTT-S Int. Microw. Symp. Dig.*, Jun. 2018, pp. 1499–1502.
- [106] F. Thome, P. Neininger, D. Schwantuschke, and R. Quay, "Broadband operation of GaN mm-Wave MMICs," in Proc. Workshop, mm-Wave GaN MMICs, 2022.
- [107] T. Sonnenberg, A. Romano, S. Verploegh, M. Pinto, and Z. Popovic, "V- and W-band millimeter-wave GaN MMICs," *IEEE J. Microw.*, vol. 3, no. 1, pp. 453–465, Jan. 2023.
- [108] K. M. K. H. Leong et al., "850 GHz receiver and transmitter front-ends using InP HEMT," *IEEE Trans. THz Sci. Technol.*, vol. 7, no. 4, pp. 466-475, Jul. 2017.

- [109] C. M. Cooke et al., "A 670 GHz integrated InP HEMT direct-detection receiver for the tropospheric water and cloud ice instrument," *IEEE Trans. THz Sci. Technol.*, vol. 11, no. 5, pp. 566–576, Sep. 2021.
- [110] G. Chattopadhyay et al., "A 340 GHz cryogenic amplifier based spectrometer for space based atmospheric science applications," in Proc. 42nd Int. Conf. Infr., Millim., THz Waves (IRMMW-THz), Aug. 2017, pp. 1–2.
- [111] T. Sonnenberg, T. Romano, S. Verploegh, and Z. Popović, "V- and W-band GaN MMIC switches," in Proc. 18th Eur. Microw. Integr. Circuits Conf. (EuMIC), Sep. 2023, pp. 257–260.
- [112] A. Romano, T. Sonnenberg, and Z. Popović, "50–110-GHz continuous GaN MMIC reflective phase shifters," *IEEE Trans. Microw. Theory Techn.*, vol. 72, no. 3, pp. 1634–1642, Mar. 2024.
- [113] T. Sonnenberg, S. Verploegh, M. Pinto, and Z. Popovic, "W-band GaN HEMT frequency multipliers," *IEEE Trans. Microw. Theory Techn.*, vol. 71, no. 10, pp. 4327–4336, Oct. 2023.
- [114] A. Romano, T. Sonnenberg, L. Marzall, and Z. Popovic, "V- through W-band GaN active circulator," in Proc. 18th

  Eur. Microw. Integr. Circuits Conf. (EuMIC),

  Sep. 2023, pp. 1–4.
- [115] A. Romano, T. Sonnenberg, and Z. Popović, "46–102 GHz GaN balanced cascode amplifier-isolator," in Proc. IEEE BICMOS Compound Semiconductor Integr. Circuits Technol. Symp. (BCICTS), Oct. 2023, pp. 211–214.
- [116] I. Mehdi, J. V. Siles, C. Lee, and E. Schlecht, "THz diode technology: Status, prospects, and applications," *Proc. IEEE*, vol. 105, no. 6, pp. 990–1007, Jun. 2017.
- [117] R. Kazarinov, "Possibility of amplification of electromagnetic waves in a semiconductor with superlattice," Sov. Phys.-Semicond., vol. 5, no. 4, pp. 707–709, 1971.
- [118] B. S. Williams, S. Kumar, Q. Hu, and J. L. Reno, "High-power terahertz quantum cascade lasers," in *Proc. Conf. Lasers Electro-Opt. Quantum Electron. Laser Sci. Conf.*, 2006, pp. 1–2.
- [119] C. Sirtori, S. Barbieri, and S. Laurent, "Amplitude modulation and stabilization of quantum-cascade lasers," SPIE Newsroom, 2010.
- [120] J. A. Fülöp, S. Tzortzakis, and T. Kampfrath, "Laser-driven strong-field terahertz sources," *Adv. Opt. Mater.*, vol. 8, no. 3, Feb. 2020, Art. no. 1900681.
- [121] A. Stohr and D. Jdger, "Photonic millimeter-wave and terahertz source technologies (invited paper)," in Proc. Int. Topical Meeting Microw. Photon., Oct. 2006, pp. 1–4.
- [122] N. M. Burford and M. O. El-Shenawee, "Review of terahertz photoconductive antenna technology," *Opt. Eng.*, vol. 56, no. 1, Jan. 2017, Art. no. 010901.
- [123] C. W. Berry, M. R. Hashemi, and M. Jarrahi, "Generation of high power pulsed terahertz radiation using a plasmonic photoconductive emitter array with logarithmic spiral antennas," Appl. Phys. Lett., vol. 104, no. 8, Feb. 2014, Art. no. 081122.
- [124] M. Dyakonov and M. Shur, "Shallow water analogy for a ballistic field effect transistor: New mechanism of plasma wave generation by DC current," Phys. Rev. Lett., vol. 71, no. 15, pp. 2465–2468, Oct. 1993.
- [125] S. A. Mikhailov, "Plasma instability and amplification of electromagnetic waves in low-dimensional electron systems," *Phys. Rev. B, Condens. Matter*, vol. 58, no. 3, pp. 1517–1532, Jul. 1998.
- [126] W. Knap et al., "Terahertz emission by plasma waves in 60 nm gate high electron mobility transistors," Appl. Phys. Lett., vol. 84, no. 13, pp. 2331–2333, Mar. 2004.
- [127] V. Ryzhii, A. Satou, and M. S. Shur, "Transit-time mechanism of plasma instability in high electron mobility transistors," *Phys. Status Solidi, A*, vol. 202, no. 10, pp. R113–R115, Aug. 2005.
- [128] A. S. Petrov, D. Svintsov, V. Ryzhii, and M. S. Shur, "Amplified-reflection plasmon instabilities in

- grating-gate plasmonic crystals," *Phys. Rev. B, Condens. Matter*, vol. 95, no. 4, Jan. 2017, Art. no. 045405.
- [129] M. Nafari and J. M. Jornet, "Modeling and performance analysis of metallic plasmonic nano-antennas for wireless optical communication in nanonetworks," *IEEE Access*, vol. 5, pp. 6389–6398, 2017.
- [130] J. Crabb, X. Cantos-Roman, J. M. Jornet, and G. R. Aizin, "Hydrodynamic theory of the Dyakonov-Shur instability in graphene transistors," *Phys. Rev. B, Condens. Matter*, vol. 104, no. 15, Oct. 2021, Art. no. 155440.
- [131] G. R. Aizin, J. Mikalopas, and M. Shur, "Plasma instability and amplified mode switching effect in THz field effect transistors with a grating gate," *Phys. Rev. B, Condens. Matter*, vol. 107, no. 24, Jun. 2023, Art. no. 245424.
- [132] J. Crabb, X. Cantos-Roman, G. R. Aizin, and J. M. Jornet, "Amplitude and frequency modulation with an on-chip graphene-based plasmonic terahertz nanogenerator," *IEEE Trans. Nanotechnol.*, vol. 21, pp. 539–546, 2022.
- [133] P. K. Singh, G. Aizin, N. Thawdar, M. Medley, and J. M. Jornet, "Graphene-based plasmonic phase modulator for terahertz-band communication," in Proc. 10th Eur. Conf. Antennas Propag. (EuCAP), Apr. 2016, pp. 1–5.
- [134] J. O. Island et al., "On-chip terahertz modulation and emission with integrated graphene junctions," *Appl. Phys. Lett.*, vol. 116, no. 16, Apr. 2020, Art. no. 161104.
- [135] P. Gopalan and B. Sensale-Rodriguez, "2D materials for terahertz modulation," Adv. Opt. Mater., vol. 8, no. 3, Feb. 2020, Art. no. 1900550.
- [136] A. N. Grigorenko, M. Polini, and K. S. Novoselov, "Graphene plasmonics," *Nature Photon.*, vol. 6, pp. 749–758, Nov. 2012.
- [137] A. Singh, M. Andrello, N. Thawdar, and J. M. Jornet, "Design and operation of a graphene-based plasmonic nano-antenna array for communication in the terahertz band," *IEEE* J. Sel. Areas Commun., vol. 38, no. 9, pp. 2104–2117, Sep. 2020.
- [138] M. S. Shur, "Terahertz plasmonic technology," IEEE Sensors J., vol. 21, no. 11, pp. 12752–12763, Jun. 2021.
- [139] C. Lin and G. Y. L. Li, "Terahertz communications: An array-of-subarrays solution," *IEEE Commun. Mag.*, vol. 54, no. 12, pp. 124–131, Dec. 2016.
- [140] S. Abu-Surra et al., "End-to-end 140 GHz wireless link demonstration with fully-digital beamformed system," in Proc. IEEE Int. Conf. Commun. Workshops, Jun. 2021, pp. 1–6.
- [141] J. Durnin, "Exact solutions for nondiffracting beams. I. The scalar theory," J. Opt. Soc. Amer. A, Opt. Image Sci., vol. 4, no. 4, pp. 651–654, Apr. 1987.
- [142] J. Durnin, J. H. Eberly, and J. J. Miceli, "Comparison of Bessel and Gaussian beams," Opt. Lett., vol. 13, no. 2, p. 79, 1988.
- [143] G. A. Siviloglou, J. Broky, A. Dogariu, and D. N. Christodoulides, "Observation of accelerating airy beams," *Phys. Rev. Lett.*, vol. 99, no. 21, Nov. 2007, Art. no. 213901.
- [144] H. Tao, A. C. Strikwerda, K. Fan, W. J. Padilla, X. Zhang, and R. D. Averitt, "Reconfigurable terahertz metamaterials," *Phys. Rev. Lett.*, vol. 103, no. 14, Oct. 2009, Art. no. 147401.
- [145] J. M. Jornet and I. F. Akyildiz, "Graphene-based nano-antennas for electromagnetic nanocommunications in the terahertz band," in Proc. 4th Eur. Conf. Antennas Propag., Apr. 2010, pp. 1–5.
- [146] M. Tamagnone, J. S. Gómez-Díaz, J. R. Mosig, and J. Perruisseau-Carrier, "Reconfigurable terahertz plasmonic antenna concept using a graphene stack," Appl. Phys. Lett., vol. 101, no. 21, Nov. 2012, Art. no. 214102.
- [147] J. M. Jornet and I. F. Akyildiz, "Graphene-based plasmonic nano-antenna for terahertz band communication in nanonetworks," *IEEE* J. Sel. Areas Commun., vol. 31, no. 12,

- pp. 685-694, Dec. 2013.
- [148] T. Gric, A. Gorodetsky, A. Trofimov, and E. Rafailov, "Tunable plasmonic properties and absorption enhancement in terahertz photoconductive antenna based on optimized plasmonic nanostructures," J. Infr., Millim., Terahertz Waves, vol. 39, no. 10, pp. 1028–1038, Oct. 2018.
- [149] I. F. Akyildiz and J. M. Jornet, "Realizing ultra-massive MIMO(1024×1024)communication in the (0.06–10) terahertz band," Nano Commun. Netw., vol. 8, pp. 46–54, Jun. 2016.
- [150] N. T. Yardimci and M. Jarrahi, "High sensitivity terahertz detection through large-area plasmonic nano-antenna arrays," Sci. Rep., vol. 7, no. 1, p. 42667, Feb. 2017.
- [151] S. E. Hosseininejad, K. Rouhi, M. Neshat, A. Cabellos-Aparicio, S. Abadal, and E. Alarcón, "Digital metasurface based on graphene: An application to beam steering in terahertz plasmonic antennas," *IEEE Trans. Nanotechnol.*, vol. 18, pp. 734–746, 2019.
- [152] A. Singh, A. J. Alqaraghuli, and J. M. Jornet, "Wavefront engineering at terahertz frequencies through intelligent reflecting surfaces," in Proc. IEEE 23rd Int. Workshop Signal Process. Adv. Wireless Commun. (SPAWC), Jul. 2022, pp. 1–5.
- [153] Q. Wu et al., "Intelligent reflecting surface-aided wireless communications: A tutorial," *IEEE Trans. Commun.*, vol. 69, no. 5, pp. 3313–3351, May 2021.
- [154] Y. Liu et al., "Reconfigurable intelligent surfaces: Principles and opportunities," *IEEE Commun. Surveys Tuts.*, vol. 23, no. 3, pp. 1546–1577, 3rd Quart., 2021.
- [155] C. Huang et al., "Holographic MIMO surfaces for 6G wireless networks: Opportunities, challenges, and trends," *IEEE Wireless Commun.*, vol. 27, no. 5, pp. 118–125, Oct. 2020.
- [156] X. Yu, D. Xu, and R. Schober, "MISO wireless communication systems via intelligent reflecting surfaces: (Invited Paper)," in Proc. IEEE/CIC Int. Conf. Commun. China (ICCC), Aug. 2019, pp. 735–740.
- [157] L. Yang, Y. Yang, M. O. Hasna, and M. Alouini, "Coverage, probability of SNR gain, and DOR analysis of RIS-aided communication systems," *IEEE Wireless Commun. Lett.*, vol. 9, no. 8, pp. 1268–1272, Aug. 2020.
- [158] B. Di, H. Zhang, L. Song, Y. Li, Z. Han, and H. V. Poor, "Hybrid beamforming for reconfigurable intelligent surface based multi-user communications: Achievable rates with limited discrete phase shifts," *IEEE J. Sel. Areas Commun*, vol. 38, no. 8, pp. 1809–1822, Aug. 2020.
- [159] A. Almohamad et al., "Smart and secure wireless communications via reflecting intelligent surfaces: A short survey," *IEEE Open J. Commun. Soc.*, vol. 1, pp. 1442–1456, Sep. 2020.
- [160] S. Nie and I. F. Akyildiz, "Beamforming in intelligent environments based on ultra-massive MIMO platforms in millimeter wave and terahertz bands," in Proc. IEEE Int. Conf. Acoust., Speech Signal Process. (ICASSP), May 2020, pp. 8683–8687.
- [161] W. Hao, F. Zhou, M. Zeng, O. A. Dobre, and N. Al-Dhahir, "Ultra wideband THz IRS communications: Applications, challenges, key techniques, and research opportunities," *IEEE Netw.*, vol. 36, no. 6, pp. 214–220, Nov. 2022.
- [162] Z. Chen, B. Ning, C. Han, Z. Tian, and S. Li, "Intelligent reflecting surface assisted terahertz communications toward 6G," *IEEE Wireless Commun.*, vol. 28, no. 6, pp. 110–117, Dec. 2021.
- [163] C. Liaskos, S. Nie, A. Tsioliaridou, A. Pitsillides, S. Ioannidis, and I. Akyildiz, "A new wireless communication paradigm through software-controlled metasurfaces," *IEEE Commun. Mag.*, vol. 56, no. 9, pp. 162–169, Sep. 2018.
- [164] F. Lan et al., "Real-time programmable metasurface for terahertz multifunctional wave front engineering," *Light, Sci. Appl.*, vol. 12, no. 1, p. 191, Aug. 2023.

- [165] A. Singh, M. Andrello, E. Einarsson, N. Thawdarl, and J. M. Jornet, "A hybrid intelligent reflecting surface with graphene-based control elements for THz communications," in Proc. IEEE 21st Int. Workshop Signal Process. Adv. Wireless
- Commun. (SPAWC), May 2020, pp. 1–5.

  [166] H. Taghvaee et al., "Multiwideband terahertz communications via tunable graphene-based metasurfaces in 6G networks: Graphene enables ultimate multiwideband THz wavefront control," IEEE Veh. Technol. Mag., vol. 17, no. 2, pp. 16–25, Jun. 2022.
- [167] S. Ju and T. S. Rappaport, "142 GHz multipath propagation measurements and path loss channel modeling in factory buildings," in *Proc. IEEE* Int. Conf. Commun., May 2023, pp. 1–6.
- [168] S. Badran, A. Singh, A. Jaiswal, E. Einarsson, and J. M. Jornet, "Design and validation of a metallic reflectarray for communications at true terahertz frequencies," in Proc. 7th ACM Workshop Millimeter-Wave THz Netw. Sens. Syst., Oct. 2023, pp. 1–10.
- [169] C. A. Balanis, Antenna Theory: Analysis and Design. Hoboken, NJ, USA: Wiley, 2016.
- [170] A. Singh et al., "Wavefront engineering: Realizing efficient terahertz band communications in 6G and beyond," *IEEE Wireless Commun.*, vol. 31, no. 3, pp. 133–139, Jun. 2024.
- [171] V. Ariyarathna, A. Madanayake, and J. M. Jornet, "Toward real-time software-defined radios for ultrabroadband communication above 100 GHz [application notes]," *IEEE Microw. Mag.*, vol. 24, no. 8, pp. 50–59, Aug. 2023.
- [172] H. Abdellatif, V. Ariyarathna, S. Petrushkevich, A. Madanayake, and J. M. Jornet, "A real-time ultra-broadband software-defined radio platform for terahertz communications," in Proc. Conf. Comput. Commun. Workshops, May 2022, pp. 1–2.
- [173] M. Matinmikko-Blue, "Research issues for sustainable wireless networks: A stakeholder approach," in Proc. 20th Int. Symp. Modeling Optim. Mobile, Ad hoc, Wireless Netw. (WiOpt), Sep. 2022, pp. 372–376.
- [174] B. Hoefflinger, "High-performance computing trends," in NANO-CHIPS 2030: On-Chip AI for an Efficient Data-Driven World. Switzerland: Springer, 2020, pp. 269–273.
- [175] O. Kanhere, H. Poddar, Y. Xing, D. Shakya, S. Ju, and T. S. Rappaport, "A power efficiency metric for comparing energy consumption in future wireless networks in the millimeter-wave and terahertz bands," *IEEE Wireless Commun.*, vol. 29, no. 6, pp. 56–63, Dec. 2022.
- [176] M. Ying, D. Shakya, H. Poddar, and T. S. Rappaport, "Waste factor: A new metric for evaluating power efficiency in any cascade," in Proc. IEEE Global Commun. Conf., Dec. 2023, pp. 1–6.
- [177] H. T. Friis, "Noise figures of radio receivers," *Proc. IRE*, vol. 32, no. 7, pp. 419–422, Jul. 1944.
- [178] T. Rappaport, M. Ying, and D. Shakya, "Waste figure and waste factor: New metrics for evaluating power efficiency in any circuit or cascade," *Microw. J.*, vol. 67, no. 5, pp. 54–84, May 2024.
- [179] T. S. Rappaport et al., "Waste factor and waste figure: A unified theory for modeling and analyzing wasted power in radio access networks for improved sustainability," *IEEE Open J. Commun.*, May 2024.
- [180] J. N. Murdock and T. S. Rappaport, "Consumption factor and power-efficiency factor: A theory for evaluating the energy efficiency of cascaded communication systems," *IEEE J. Sel. Areas Commun.*, vol. 32, no. 2, pp. 221–236, Feb. 2014.
- [181] C. Han et al., "Terahertz wireless channels: A holistic survey on measurement, modeling, and analysis," *IEEE Commun. Surveys Tuts.*, vol. 24, no. 3, pp. 1670–1707, 3rd Quart., 2022.
- [182] A. Ghosh and M. Kim, "THz channel sounding and modeling techniques: An overview," *IEEE Access*, vol. 11, pp. 17823–17856, 2023.
- [183] S. Sun, G. R. MacCartney, M. K. Samimi, and T. S. Rappaport, "Synthesizing omnidirectional antenna patterns, received power and path loss

- from directional antennas for 5G millimeter-wave communications," in *Proc. IEEE Glob. Commun. Conf. (GLOBECOM)*, May 2015, pp. 1–7.
- [184] T. S. Rappaport, Y. Qiao, J. I. Tamir, J. N. Murdock, and E. Ben-Dor, "Cellular broadband millimeter wave propagation and angle of arrival for adaptive beam steering systems," in *Proc. IEEE Radio Wireless Symp.*, Jan. 2012, pp. 151–154.
- [185] M. K. Samimi and T. S. Rappaport, "Statistical channel model with multi-frequency and arbitrary antenna beamwidth for millimeter-wave outdoor communications," in Proc. IEEE Globecom Workshops, Dec. 2015, pp. 1–7.
- [186] Y. Xing, T. S. Rappaport, and A. Ghosh, "Millimeter wave and sub-THz indoor radio propagation channel measurements, models, and comparisons in an office environment," *IEEE Commun. Lett.*, vol. 25, no. 10, pp. 3151–3155, Oct. 2021.
- [187] T. S. Rappaport, Wireless Communications: Principles and Practice, 2/E. Upper Saddle River, NJ, USA: Prentice-Hall, 2002.
- 188] T. Kurner, R. Piesiewicz, M. Koch, and J. Schoebel, "Propagation models, measurements and simulations for wireless communication systems beyond 100 GHz," in Proc. Int. Conf. Electromagn. Adv. Appl., Sep. 2007, pp. 108–111.
- [189] J. M. Jornet and I. F. Akyildiz, "Channel modeling and capacity analysis for electromagnetic wireless nanonetworks in the terahertz band," *IEEE Trans. Wireless Commun.*, vol. 10, no. 10, pp. 3211–3221, Oct. 2011.
- [190] S. Tarboush et al., "TeraMIMO: A channel simulator for wideband ultra-massive MIMO terahertz communications," *IEEE Trans. Veh. Technol.*, vol. 70, no. 12, pp. 12325–12341, Dec. 2021.
- [191] H. Yi et al., "Ray tracing meets terahertz: Challenges and opportunities," *IEEE Commun. Mag.*, vol. 62, no. 2, pp. 40–46, Feb. 2024.
- [192] J. Zhang et al., "Deterministic ray tracing: A promising approach to THz channel modeling in 6G deployment scenarios," *IEEE Commun. Mag.*, vol. 62, no. 2, pp. 48–54, Feb. 2024.
- [193] M. K. Samimi and T. S. Rappaport, "3-D millimeter-wave statistical channel model for 5G wireless system design," *IEEE Trans. Microw. Theory Techn.*, vol. 64, no. 7, pp. 2207–2225, Jul. 2016.
- [194] G. R. MacCartney and T. S. Rappaport, "Rural macrocell path loss models for millimeter wave wireless communications," *IEEE J. Sel. Areas Commun.*, vol. 35, no. 7, pp. 1663–1677, Jul 2017
- [195] T. S. Rappaport, Y. Xing, G. R. MacCartney, A. F. Molisch, E. Mellios, and J. Zhang, "Overview of millimeter wave communications for fifth-generation (5G) wireless networks—With a focus on propagation models," *IEEE Trans. Antennas Propag.*, vol. 65, no. 12, pp. 6213–6230, Dec. 2017.
- [196] C. Han and Y. Chen, "Propagation modeling for wireless communications in the terahertz band," *IEEE Commun. Mag.*, vol. 56, no. 6, pp. 96–101, Jun. 2018.
- [197] M. Shafi et al., "5G: A tutorial overview of standards, trials, challenges, deployment, and practice," *IEEE J. Sel. Areas Commun.*, vol. 35, no. 6, pp. 1201–1221, Jun. 2017.
- [198] N. A. Abbasi et al., "THz band channel measurements and statistical modeling for urban D2D environments," *IEEE Trans. Wireless Commun.*, vol. 22, no. 3, pp. 1466–1479, Mar. 2023.
- [199] F. Sheikh et al., "THz measurements, antennas, and simulations: From the past to the future," *IEEE J. Microw.*, vol. 3, no. 1, pp. 289–304, Jan. 2023.
- [200] K. Guan et al., "Channel characterization for intra-wagon communication at 60 and 300 GHz bands," *IEEE Trans. Veh. Technol.*, vol. 68, no. 6, pp. 5193–5207, Jun. 2019.
- [201] S. Sun, T. S. Rappaport, M. Shafi, P. Tang,

- J. Zhang, and P. J. Smith, "Propagation models and performance evaluation for 5G millimeter-wave bands," *IEEE Trans. Veh. Technol.*, vol. 67, no. 9, pp. 8422–8439, Sep. 2018.
- [202] G. R. MacCartney and T. S. Rappaport, "A flexible millimeter-wave channel sounder with absolute timing," *IEEE J. Sel. Areas Commun.*, vol. 35, no. 6, pp. 1402–1418, Jun. 2017.
- [203] H. Poddar, S. Ju, D. Shakya, and T. S. Rappaport, "A tutorial on NYUSIM: Sub-terahertz and millimeter-wave channel simulator for 5G, 6G and beyond," *IEEE Commun. Surveys Tuts.*, vol. 26, no. 2, pp. 824–857, 2nd Quart., 2023.
- [204] K. Dovelos, S. D. Assimonis, H. Q. Ngo, B. Bellalta, and M. Matthaiou, "Intelligent reflecting surfaces at terahertz bands: Channel modeling and analysis," in Proc. IEEE Int. Conf. Commun. Workshops (ICC Workshops), Jun. 2021, pp. 1–6.
- [205] R. M. Goody and Y. L. Yung, Atmospheric Radiation: Theoretical Basis. Cambridge, U.K.: Cambridge Univ. Press, 1995.
- [206] V. Petrov, M. Komarov, D. Moltchanov, J. M. Jornet, and Y. Koucheryavy, "Interference analysis of EHF/THF communications systems with blocking and directional antennas," in Proc. IEEE Global Commun. Conf. (GLOBECOM), Dec. 2016, pp. 1–7.
- [207] J. Kokkoniemi, J. Lehtomäki, V. Petrov, D. Moltchanov, and M. Juntti, "Frequency domain penetration loss in the terahertz band," in Proc. Global Symp. Millim. Waves (GSMM) ESA Workshop Millimetre-Wave Technol. Appl., Jun. 2016, pp. 1–4.
- [208] V. Petrov, M. Komarov, D. Moltchanov, J. M. Jornet, and Y. Koucheryavy, "Interference and SINR in millimeter wave and terahertz communication systems with blocking and directional antennas," *IEEE Trans. Wireless Commun.*, vol. 16, no. 3, pp. 1791–1808, Mar. 2017.
- [209] J. Kokkoniemi, J. M. Jornet, V. Petrov, Y. Koucheryavy, and M. Juntti, "Channel modeling and performance analysis of airplane-satellite terahertz band communications," *IEEE Trans. Veh. Technol.*, vol. 70, no. 3, pp. 2047–2061, Mar. 2021.
- [210] P. Boronin, V. Petrov, D. Moltchanov, Y. Koucheryavy, and J. M. Jornet, "Capacity and throughput analysis of nanoscale machine communication through transparency windows in the terahertz band," Nano Commun. Netw., vol. 5, no. 3, pp. 72–82, Sep. 2014.
- [211] V. Petrov, D. Moltchanov, and Y. Koucheryavy, "On the efficiency of spatial channel reuse in ultra-dense THz networks," in *Proc. IEEE Global Commun. Conf. (GLOBECOM)*, Dec. 2015, pp. 1–7.
- [212] M. Marcus, X. C. Roman, and J. Jornet, "Millimeter-wave propagation: Spectrum management implications-an update for >100 GHz [speaker's corner]," *IEEE Microw. Mag.*, vol. 24, no. 1, pp. 91–94, May 2022.
- [213] C. Han, W. Gao, N. Yang, and J. M. Jornet, "Molecular absorption effect: A double-edged sword of terahertz communications," *IEEE Wireless Commun.*, vol. 30, no. 4, pp. 140–146, Jun. 2023.
- [214] J. M. Jornet and I. F. Akyildiz, "Femtosecond-long pulse-based modulation for terahertz band communication in nanonetworks," *IEEE Trans. Commun.*, vol. 62, no. 5, pp. 1742–1754, May 2014.
- [215] J. Kokkoniemi, J. Lehtomäki, and M. Juntti, "A discussion on molecular absorption noise in the terahertz band," *Nano Commun. Netw.*, vol. 8, pp. 35–45, Jun. 2016.
- [216] V. Petrov, D. Moltchanov, Y. Koucheryavy, and J. M. Jornet, "Capacity and outage of terahertz communications with user micro-mobility and beam misalignment," *IEEE Trans. Veh. Technol.*, vol. 69, no. 6, pp. 6822–6827, Jun. 2020.
- [217] J. Kokkoniemi, J. Lehtomäki, K. Umebayashi, and M. Juntti, "Frequency and time domain channel models for nanonetworks in terahertz band," *IEEE Trans. Antennas Propag.*, vol. 63, no. 2, pp. 678–691, Feb. 2015.
- [218] J. Kokkoniemi, P. Rintanen, J. Lehtomaki, and

- M. Juntti, "Diffraction effects in terahertz band—Measurements and analysis," in *Proc. IEEE Global Commun. Conf. (GLOBECOM)*, Dec. 2016, pp. 1–6.
- [219] A. Al-Saman, M. Cheffena, O. Elijah, Y. A. Al-Gumaei, S. K. A. Rahim, and T. Al-Hadhrami, "Survey of millimeter-wave propagation measurements and models in indoor environments," *Electronics*, vol. 10, no. 14, p. 1653, Jul. 2021. [Online]. Available: https://www.mdpi.com/2079-9292/10/14/1653
- [220] C.-X. Wang, J. Bian, J. Sun, W. Zhang, and M. Zhang, "A survey of 5G channel measurements and models," *IEEE Commun. Surveys Tuts.*, vol. 20, no. 4, pp. 3142–3168, 4th Quart., 2018.
- [221] Y. Chen, Y. Li, C. Han, Z. Yu, and G. Wang, "Channel measurement and ray-tracing-statistical hybrid modeling for low-terahertz indoor communications," *IEEE Trans. Wireless Commun.*, vol. 20, no. 12, pp. 8163–8176, Dec. 2021.
- [222] Y. Chen, C. Han, Z. Yu, and G. Wang, "Channel measurement, characterization and modeling for terahertz indoor communications above 200 GHz," *IEEE Trans. Wireless Commun.*, early access, Nov. 22, 2024, doi: 10.1109/TWC.2023.3333222.
- [223] C. Jansen et al., "Diffuse scattering from rough surfaces in THz communication channels," *IEEE Trans. THz Sci. Technol.*, vol. 1, no. 2, pp. 462–472, Nov. 2011.
- [224] S. Ju et al., "Scattering mechanisms and modeling for terahertz wireless communications," in Proc. IEEE Int. Conf. Commun. (ICC), May 2019, pp. 1–7.
- [225] C.-L. Cheng and A. Zajic, "Characterization of propagation phenomena relevant for 300 GHz wireless data center links," *IEEE Trans. Antennas Propag.*, vol. 68, no. 2, pp. 1074–1087, Feb. 2020.
- [226] C. Slezak, V. Semkin, S. Andreev, Y. Koucheryavy, and S. Rangan, "Empirical effects of dynamic human-body blockage in 60 GHz communications," *IEEE Commun. Mag.*, vol. 56, no. 12, pp. 60–66, Dec. 2018.
- [227] M. Gapeyenko et al., "On the temporal effects of mobile blockers in urban millimeter-wave cellular scenarios," *IEEE Trans. Veh. Technol.*, vol. 66, no. 11, pp. 10124–10138, Nov. 2017.
- [228] M. Gapeyenko et al., "Analysis of human-body blockage in urban millimeter-wave cellular communications," in Proc. IEEE Int. Conf. Commun. (ICC), May 2016, pp. 1–7.
- [229] F. Mokhtari-Koushyar, M. Alamdar, and M. Fakharzadeh, "Human body scattering modeling and measurement for millimeter-wave and 5G bands," in Proc. IEEE Texas Symp. Wireless Microw. Circuits Syst. (WMCS), Mar. 2019, pp. 1–5.
- [230] T. Bai and R. W. Heath Jr., "Analysis of self-body blocking effects in millimeter wave cellular networks," in Proc. 48th Asilomar Conf. Signals, Syst. Comput., Nov. 2014, pp. 1921–1925.
- [231] S. H. A. Samy, E. A. Maher, A. El-Mahdy, and F. Dressler, "Power optimization of THz band heterogeneous vehicular networks," in *Proc. IEEE Veh. Netw. Conf. (VNC)*, Nov. 2021, pp. 107–114.
- [232] J. M. Eckhardt, V. Petrov, D. Moltchanov, Y. Koucheryavy, and T. Kurner, "Channel measurements and modeling for low-terahertz band vehicular communications," *IEEE* J. Sel. Areas Commun., vol. 39, no. 6, pp. 1590–1603, Jun. 2021.
- [233] R. Schneider, D. Didascalou, and W. Wiesbeck, "Impact of road surfaces on millimeter-wave propagation," *IEEE Trans. Veh. Technol.*, vol. 49, no. 4, pp. 1314–1320, Jul. 2000.
- [234] V. Petrov, J. M. Eckhardt, D. Moltchanov, Y. Koucheryavy, and T. Kürner, "Measurements of reflection and penetration losses in low terahertz band vehicular communications," in Proc. 14th Eur. Conf. Antennas Propag. (EuCAP), Mar. 2020, pp. 1–5.
- [235] C. Tunc and S. S. Panwar, "Mitigating the impact of blockages in millimeter-wave vehicular networks through vehicular relays," *IEEE Open J. Intell. Transp. Syst.*, vol. 2, pp. 225–239, 2021.

- [236] V. Petrov, D. Moltchanov, S. Andreev, and R. W. Heath Jr., "Analysis of intelligent vehicular relaying in urban 5G+ millimeter-wave cellular deployments," in Proc. IEEE Global Commun. Conf. (GLOBECOM), Dec. 2019, pp. 1–6.
- [237] S. Ju, Y. Xing, O. Kanhere, and T. S. Rappaport, "Millimeter wave and sub-terahertz spatial statistical channel model for an indoor office building," *IEEE J. Sel. Areas Commun.*, vol. 39, no. 6, pp. 1561–1575, Jun. 2021.
- [238] T. Doeker, J. M. Eckhardt, and T. Kürner, "Channel measurements and modeling for low terahertz communications in an aircraft cabin," *IEEE Trans. Antennas Propag.*, vol. 70, no. 11, pp. 10903–10916, Nov. 2022.
- [239] C. Han, A. O. Bicen, and I. F. Akyildiz, "Multi-ray channel modeling and wideband characterization for wireless communications in the terahertz band," *IEEE Trans. Wireless Commun.*, vol. 14, no. 5, pp. 2402–2412, May 2015.
- [240] D. Bodet, P. Dinh, M. Stojanovic, J. Widmer, D. Koutsonikolas, and J. M. Jornet, "Characterizing sub-THz MIMO channels in practice: A novel channel sounder with absolute time reference," in Proc. IEEE Global Commun. Conf., Dec. 2023, pp. 1459–1464.
- [241] S. Ju, D. Shakya, H. Poddar, Y. Xing, O. Kanhere, and T. S. Rappaport, "142 GHz sub-terahertz radio propagation measurements and channel characterization in factory buildings," *IEEE Trans. Wireless Commun.*, early access, Dec. 6, 2023, doi: 10.1109/TWC.2023.3337601.
- [242] Technical Specification Group Radio Access Network: Study on Channel Model for Frequencies From 0.5 to 100 GHz (Release 16), document TR 38.901. 3GPP 2019.
- [243] S. Latini, K. T. Winther, T. Olsen, and K. S. Thygesen, "Interlayer excitons and band alignment in MoS2/hBN/WSe2 van der Waals heterostructures," Nano Lett., vol. 17, no. 2, pp. 938–945, Feb. 2017.
- [244] M. G. Burdanova et al., "Ultrafast optoelectronic processes in 1D radial van der Waals heterostructures: Carbon, boron nitride, and MoS<sub>2</sub> nanotubes with coexisting excitons and highly mobile charges," Nano Lett., vol. 20, no. 5, pp. 3560–3567, May 2020.
- [245] J. Park and H. Wang, "A 26-to-39GHz broadband ultra-compact high-linearity switchless hybrid N/PMOS bi-directional PA/LNA front-end for multi-band 5G large-scaled MIMO system," in IEEE Int. Solid-State Circuits Conf. (ISSCC) Dig. Tech. Papers, vol. 65, Feb. 2022, pp. 322–324.
- [246] I. Abdo et al., "22.2 A 300 GHz-band phased-array transceiver using bi-directional outphasing and Hartley architecture in 65 nm CMOS," in IEEE Int. Solid-State Circuits Conf. (ISSCC) Dig. Tech. Papers, vol. 64, Feb. 2021, pp. 316–318.
- [247] B. A. Abdelmagid and H. Wang, "An ultra-compact and wideband transformer-based coupler with arbitrary phase difference and arbitrary power division ratio," *IEEE Trans. Microw. Theory Techn.*, vol. 72, no. 2, pp. 1133–1147, Feb. 2024.
- [248] B. Ning et al., "Beamforming technologies for ultra-massive MIMO in terahertz communications," *IEEE Open J. Commun. Soc.*, vol. 4, pp. 614–658, 2023.
- [249] H. Wang, H. Mohammadnezhad, and P. Heydari, "Analysis and design of high-order QAM direct-modulation transmitter for high-speed point-to-point mm-wave wireless links," *IEEE J. Solid-State Circuits*, vol. 54, no. 11, pp. 3161–3179, Nov. 2019.
- [250] J. S. Chien and J. F. Buckwalter, "A 110–120-GHz, 12.2% efficiency, 16.2-dBm output power multiplying outphasing transmitter in 22-nm FDSOI," in Proc. IEEE Asian Solid-State Circuits Conf. (A-SSCC), Nov. 2022, pp. 1–3.
- [251] C. D'Heer and P. Reynaert, "A 135 GHz 32 Gb/s direct-digital modulation 16-QAM transmitter in 28 nm CMOS," in Proc. IEEE 48th Eur. Solid State Circuits Conf. (ESSCIRC), Sep. 2022, pp. 481–484.
- [252] M. U. Rehman, S. Ravichandran, S. Erdogan, and M. Swaminathan, "W-band and D-band transmission lines on glass based substrates for

- sub-THz modules," in *Proc. IEEE 70th Electron. Compon. Technol. Conf. (ECTC)*, Jun. 2020, pp. 660–665.
- [253] A. Singh et al., "A D-band radio-on-glass module for spectrally-efficient and low-cost wireless backhaul," in Proc. IEEE Radio Freq. Integr. Circuits Symp. (RFIC), Aug. 2020, pp. 99–102, doi: 10.1109/RFIC49505.2020.9218437.
- [254] M. Elkhouly et al., "Fully integrated 2D scalable TX/RX chipset for D-band phased-array-on-glass modules," in *IEEE Int. Solid-State Circuits* Conf. (ISSCC) Dig. Tech. Papers, vol. 65, Feb. 2022, pp. 76–78.
- [255] M. Cui, Z. Wu, Y. Lu, X. Wei, and L. Dai, "Near-field MIMO communications for 6G: Fundamentals, challenges, potentials, and future directions," *IEEE Commun. Mag.*, vol. 61, no. 1, pp. 40–46, Jan. 2023.
- [256] E. Björnson and L. Sanguinetti, "Power scaling laws and near-field behaviors of massive MIMO and intelligent reflecting surfaces," *IEEE Open* J. Commun. Soc., vol. 1, pp. 1306–1324, 2020.
- [257] I. V. A. K. Reddy, D. Bodet, A. Singh, V. Petrov, C. Liberale, and J. M. Jornet, "Ultrabroadband terahertz-band communications with self-healing Bessel beams," Commun. Eng., vol. 2, no. 1, pp. 1–10, Oct. 2023.
- [258] V. Petrov, D. Bodet, and A. Singh, "Mobile near-field terahertz communications for 6G and 7G networks: Research challenges," Frontiers Commun. Netw., vol. 4, Mar. 2023, Art. no. 1151324.
- [259] V. Petrov, J. M. Jornet, and A. Singh, "Near-field 6G networks: Why mobile terahertz communications MUST operate in the near field," in Proc. IEEE Global Commun. Conf., Dec. 2023, pp. 3983–3989.
- [260] P. Sen, S. Badran, V. Petrov, A. Singh, and J. M. Jornet, "Impact of the antenna on the sub-terahertz indoor channel characteristics: An experimental approach," 2024, arXiv:2403.04168.
- [261] V. Petrov, H. Guerboukha, D. M. Mittleman, and A. Singh, "Wavefront hopping: An enabler for reliable and secure near field terahertz communications in 6G and beyond," *IEEE Wireless Commun.*, vol. 31, no. 1, pp. 48–55, Feb. 2024.
- [262] R. Singh and D. Sicker, "Parameter modeling for small-scale mobility in indoor THz communication," in Proc. IEEE Global Commun. Conf. (GLOBECOM), Dec. 2019, pp. 1–6.
- [263] Y. Li, Y. Wang, Y. Chen, Z. Yu, and C. Han, "Channel measurement and analysis in an indoor corridor scenario at 300 GHz," in Proc. IEEE Int. Conf. Commun., May 2022, pp. 2888–2893.
- [264] T. S. Rappaport, S. Sun, and M. Shafi, "Investigation and comparison of 3GPP and NYUSIM channel models for 5G wireless communications," in *Proc. IEEE 86th* Veh. Technol. Conf. (VTC-Fall), Sep. 2017, pp. 1–5.
- [265] Z. Yu, Y. Chen, G. Wang, W. Gao, and C. Han, "Wideband channel measurements and temporal-spatial analysis for terahertz indoor communications," in Proc. IEEE Int. Conf. Commun. Workshops (ICC Workshops), Jun. 2020, pp. 1–6.
- [266] O. Kanhere and T. S. Rappaport, "Calibration of NYURay, a 3D mmWave and sub-THz ray tracer using indoor, outdoor, and factory channel measurements," in *Proc. IEEE Int. Conf. Commun.*, May 2023, pp. 1–10.
- [267] Z. Hossain, Q. Xia, and J. M. Jornet, "TeraSim: An ns-3 extension to simulate terahertz-band communication networks," *Nano Commun. Netw.*, vol. 17, pp. 36–44, Sep. 2018.
- [268] A. A. Gargari, M. Polese, and M. Zorzi, "Full-stack comparison of channel models for networks above 100 GHz in an indoor scenario," in Proc. 5th ACM Workshop Millimeter-Wave THz Netw. Sens. Syst., Oct. 2021, pp. 43–48.
- [269] M. Polese, J. M. Jornet, T. Melodia, and M. Zorzi, "Toward end-to-end, full-stack 6G terahertz networks," *IEEE Commun. Mag.*, vol. 58, no. 11, pp. 48–54, Nov. 2020.
- [270] A. A. Gargari, M. Pagin, M. Polese, and M. Zorzi,

- "6G integrated access and backhaul networks with sub-terahertz links," in *Proc. 18th Wireless Demand Netw. Syst. Services Conf. (WONS)*, Jan. 2023, pp. 13–19.
- [271] A. A. Gargari, M. Pagin, A. Ortiz, N. M. Gholian, M. Polese, and M. Zorzi, "Demo: [SeBaSi] system-level integrated access and backhaul simulator for self-backhauling," in Proc. IEEE 24th Int. Symp. World Wireless, Mobile Multimedia Netw. (WoWMoM), Jun. 2023, pp. 355–357.
- [272] P. Sen, V. Ariyarathna, A. Madanayake, and J. M. Jornet, "A versatile experimental testbed for ultrabroadband communication networks above 100 GHz," *Comput. Netw.*, vol. 193, Jul. 2021, Art. no. 108092.
- [273] FCC. FCC Online Table of Frequency Allocations. Accessed: Apr. 1, 2024. [Online]. Available: http://transition.fcc.gov/oet/spectrum/ table/fcctable.pdf
- [274] M. Polese et al., "Coexistence and spectrum sharing above 100 GHz," Proc. IEEE, vol. 111, no. 8, pp. 928–954, Aug. 2023.
- [275] L. Moeller, J. Federici, and K. Su, "2.5 Gbit/s duobinary signalling with narrow bandwidth 0.625 terahertz source," *Electron. Lett.*, vol. 47, no. 15, p. 856, 2011.
- [276] S. Tarboush, H. Sarieddeen, M.-S. Alouini, and T. Y. Al-Naffouri, "Single-versus multicarrier terahertz-band communications: A comparative study," *IEEE Open J. Commun. Soc.*, vol. 3, pp. 1466–1486, 2022.
- [277] P. Desombre, H. Farès, and Y. Louet, "Performance comparison of digital modulations in the presence of Gaussian phase noise in the sub-THz context," in Proc. 4th Int. Workshop Mobile THz Syst. (IWMTS), Jul. 2021, pp. 1–5.
- [278] M. Jian and R. Liu, "Baseband signal processing for terahertz: Waveform design, modulation and coding," in Proc. Int. Wireless Commun. Mobile Comput. (IWCMC), Jun. 2021, pp. 1710–1715.
- [279] C. T. Parisi, S. Badran, P. Sen, V. Petrov, and J. M. Jornet, "Modulations for terahertz band communications: Joint analysis of phase noise impact and PAPR effects," *IEEE Open* J. Commun. Soc., vol. 5, pp. 412–429, 2024.
- [280] C. Bosso, P. Sen, X. Cantos-Roman, C. Parisi, N. Thawdar, and J. M. Jornet, "Ultrabroadband spread spectrum techniques for secure dynamic spectrum sharing above 100 GHz between active

- and passive users," in *Proc. IEEE*Int. Symp. Dyn. Spectr. Access Netw. (DySPAN),
  Dec. 2021, pp. 45–52.
- [281] C. Han and I. F. Akyildiz, "Distance-aware multi-carrier (DAMC) modulation in terahertz band communication," in *Proc. IEEE Int. Conf. Commun. (ICC)*, Jun. 2014, pp. 5461–5467.
- [282] D. Bodet, P. Sen, Z. Hossain, N. Thawdar, and J. M. Jornet, "Hierarchical bandwidth modulations for ultra-broadband communications in the terahertz band," *IEEE Trans. Wireless Commun.*, vol. 22, no. 3, pp. 1931–1947, Mar. 2023.
- [283] J. M. Jornet and I. F. Akyildiz, "Low-weight channel coding for interference mitigation in electromagnetic nanonetworks in the terahertz band," in *Proc. IEEE Int. Conf. Commun. (ICC)*, Oct. 2011, pp. 1–6.
- [284] M. Kocaoglu and O. B. Akan, "Minimum energy channel codes for nanoscale wireless communications," *IEEE Trans. Wireless Commun.*, vol. 12, no. 4, pp. 1492-1500, Apr. 2013.
- vol. 12, no. 4, pp. 1492–1500, Apr. 2013.

  [285] N. Akkari et al., "Joint physical and link layer error control analysis for nanonetworks in the terahertz band," Wireless Netw., vol. 22, no. 4, pp. 1221–1233, May 2016.
- [286] T. S. Rappaport, R. W. Heath Jr., R. C. Daniels, and J. N. Murdock, Millimeter Wave Wireless Communications. London, U.K.: Pearson, 2015.
- [287] S. Sun, T. S. Rappaport, M. Shafi, and H. Tataria, "Analytical framework of hybrid beamforming in multi-cell millimeter-wave systems," *IEEE Trans. Wireless Commun.*, vol. 17, no. 11, pp. 7528–7543, Nov. 2018.
- [288] A. Alkhateeb, O. El Ayach, G. Leus, and R. W. Heath, "Channel estimation and hybrid precoding for millimeter wave cellular systems," *IEEE J. Sel. Topics Signal Process.*, vol. 8, no. 5, pp. 831–846, Oct. 2014.
- [289] M. Kanaka Chary, C. H. Vamshi Krishna, and D. Rama Krishna, "Accurate channel estimation and hybrid beamforming using artificial intelligence for massive MIMO 5G systems," AEU-Int. J. Electron. Commun., vol. 173, Jan. 2024, Art. no. 154971.
- [290] Y. Ghasempour, C.-Y. Yeh, R. Shrestha, D. Mittleman, and E. Knightly, "Single shot single antenna path discovery in THz networks," in

- Proc. 26th Annu. Int. Conf. Mobile Comput. Netw., New York, NY, USA, Apr. 2020, pp. 1–13.
- [291] N. S. Mannem, J. Park, E. Erfani, E. Liu, J. Lee and H. Wang, "A reconfigurable phase-time array transmitter achieving keyless secured transmission and multi-receiver localization for low-latency joint communication and sensing," *IEEE J. Solid-State Circuits*, vol. 58, no. 7, pp. 1898–1912, Jul. 2023, doi: 10.1109/JSSC.2023.3237462.
- [292] N. S. Mannem, E. Erfani, T.-Y. Huang, and H. Wang, "A mm-wave frequency modulated transmitter array for superior resolution in angular localization supporting low-latency joint communication and sensing," *IEEE J. Solid-State Circuits*, vol. 58, no. 6, pp. 1572–1585, Jun. 2023, doi: 10.1109/JSSC.2022.3212207.
- [293] A. Faisal, H. Sarieddeen, H. Dahrouj, T. Y. Al-Naffouri, and M.-S. Alouini, "Ultramassive MIMO systems at terahertz bands: Prospects and challenges," *IEEE Veh. Technol. Mag.*, vol. 15, no. 4, pp. 33–42, Dec. 2020.
- [294] H. Do, S. Cho, J. Park, H.-J. Song, N. Lee, and A. Lozano, "Terahertz line-of-sight MIMO communication: Theory and practical challenges," *IEEE Commun. Mag.*, vol. 59, no. 3, pp. 104–109, Mar. 2021.
- [295] H. Lu et al., "A tutorial on near-field XL-MIMO communications towards 6G," IEEE Commun. Surveys Tuts., early access, 2024
- [296] D. M. Bodet and J. M. Jornet, "Directional antennas for sub-THz and THz MIMO systems: Bridging the gap between theory and implementation," *IEEE Open J. Commun. Soc.*, vol. 4, pp. 2261–2273, 2023.
- [297] S. Elhoushy, M. Ibrahim, and W. Hamouda, "Cell-free massive MIMO: A survey," *IEEE Commun. Surveys Tuts.*, vol. 24, no. 1, pp. 492–523, 1st Ouart., 2022.
- [298] B. Li et al., "MDD-enabled two-tier terahertz fronthaul in indoor industrial cell-free massive MIMO," *IEEE Trans. Commun.*, vol. 72, no. 3, pp. 1653–1670, Mar. 2024.
- [299] M. A. Saeidi, H. Tabassum, and M.-S. Alouini, "Multi-band wireless networks: Architectures, challenges, and comparative analysis," *IEEE Commun. Mag.*, vol. 62, no. 1, pp. 80–86, Jan. 2024.

#### ABOUT THE AUTHORS

Josep M. Jornet (Fellow, IEEE) received the Bachelor of Science degree in telecommunication engineering and the Master of Science degree in information and communication technologies from the Universitat Politècnica de Catalunya, Barcelona, Spain, in 2008, and the Ph.D. degree in electrical and computer engineering from Georgia Institute of Technology, Atlanta, GA, in August 2013.



From August 2013 to August 2019, he was with the Department of Electrical Engineering, University at Buffalo (UB), The State University of New York (SUNY), Buffalo, NY, USA. He is currently a Professor with the Department of Electrical and Computer Engineering, the Director of the Ultrabroadband Nanonetworking (UN) Laboratory, and the Associate Director of the Institute for the Wireless Internet of Things, Northeastern University (NU), Boston, MA, USA. He is a leading expert in terahertz communications, in addition to wireless nano- and bio-communication networks and the Internet of Nano-Things. In these areas, he has coauthored more than 250 peerreviewed scientific publications, including one book, and has been granted five U.S. patents. His work has received over 17 000 citations (H-index of 61 since June 2024). He is serving as the lead Principal Investigator on multiple grants from U.S. federal agencies, including the National Science Foundation, the Air Force Office of Scientific Research, and the Air Force Research Laboratory as well as industry.

Dr. Jornet was a recipient of multiple awards, including the 2017 IEEE ComSoc Young Professional Best Innovation Award, the 2017 ACM NanoCom Outstanding Milestone Award, the NSF CAREER Award in 2019, the 2022 IEEE ComSoc RCC Early Achievement Award, and the 2022 IEEE Wireless Communications Technical Committee Outstanding Young Researcher Award; and four best paper awards. He has been an IEEE ComSoc Distinguished Lecturer since 2022. He is the Editor-in-Chief of Nano Communication Networks (Elsevier) and an Editor of IEEE TRANSACTIONS ON COMMUNICATIONS and Scientific Reports (Nature).

**Vitaly Petrov** (Member, IEEE) received the M.Sc. degree in information systems security from SUAI University, St. Petersburg, Russia, in 2011, the M.Sc. degree in IT and communications engineering from Tampere University of Technology, Tampere, Finland, in 2014, and the Ph.D. degree in communications engineering from Tampere University, Tampere, in 2020.



He is currently an Assistant Professor with the Division of Communication Systems, KTH Royal Institute of Technology, Stockholm, Sweden. Prior to joining KTH in 2024, he was a Principal Research Scientist at Northeastern University, Boston, MA, USA, from 2022

to 2024, and a Senior Standardization Specialist and a 3GPP RAN1 delegate with Nokia Bell Labs, Murray Hill, NJ, USA, and later Nokia Standards, Espoo, Finland, from 2020 to 2022. He has been a Visiting Researcher with The University of Texas at Austin, Austin, TX, USA; Georgia Institute of Technology, Atlanta, GA, USA; and King's College London, London, U.K. His current research interests include terahertz band communications and networking.

Dr. Petrov was a recipient of the Best Student Paper Award at IEEE VTC-Fall 2015, the Best Student Poster Award at IEEE WCNC 2017, and the Best Student Journal Paper Award from IEEE Finland in 2019.

Hua Wang (Fellow, IEEE) received the M.S. and Ph.D. degrees in electrical engineering from California Institute of Technology, Pasadena, CA, USA, in 2007 and 2009, respectively.

He was a tenured Associate Professor at the School of Electrical and Computer Engineering (ECE), Georgia Institute of Technology (Georgia Tech), Atlanta, GA, USA. He

held the Demetrius T. Paris Professorship at Georgia Tech. He was the Director of the Georgia Tech Electronics and Micro-System (GEMS) Laboratory. He worked at Intel Corporation, Hillsboro, OR, USA, and Skyworks Solutions, Campbell, CA, USA, from 2010 to 2011. He is currently a Full Professor and the Chair of Electronics at the Department of Information Technology and Electrical Engineering (D-ITET), Swiss Federal Institute of Technology Zürich (ETH Zürich), Zürich, Switzerland. He is also the Institute Deputy Head of the Integrated Systems Laboratory (IIS), ETH Zürich, and the Director of the ETH Integrated Devices, Electronics, And Systems (IDEAS) Group. He is a Faculty Member of the ETH Zürich Quantum Center. He has authored or coauthored over 250 peer-reviewed journal articles and conference papers. He is interested in innovating analog, mixed-signal, RF, and millimeter-wave (mm-Wave) integrated circuits and hybrid systems for wireless communication, sensing, and bioelectronics applications.

Dr. Wang was a Technical Program Committee (TPC) Member of IEEE International Solid-State Circuits Conference (ISSCC), Radio Frequency Integrated Circuits Symposium (RFIC) and Custom Integrated Circuits Conference (CICC). He was a Top Contributing Author to IEEE ISSCC for the past 70 years for the term of 1954-2023. He received the DARPA Director's Fellowship Award in 2020 (the first awardee in Georgia Tech's history), the DARPA Young Faculty Award in 2018, the National Science Foundation CAREER Award in 2015, the Qualcomm Faculty Award in 2020 and 2021, the IEEE MTT-S Outstanding Young Engineer Award in 2017, the Georgia Tech Sigma Xi Young Faculty Award in 2016, the Georgia Tech ECE Outstanding Junior Faculty Member Award in 2015, and the Lockheed Dean's Excellence in Teaching Award in 2015. His research group has won multiple academic awards and best paper awards, including the 2019 Marconi Society Paul Baran Young Scholar; and Best Student Paper Awards at IEEE RFIC, CICC, IMS Conferences. He was a Distinguished Lecturer (DL) of the IEEE Solid-State Circuits Society (SSCS) from 2018 to 2019. He is a Distinguished Microwave Lecturer (DML) of the IEEE Microwave Theory and Techniques Society (MTT-S) for the term of 2022–2024.

Zoya Popović (Fellow, IEEE) received the Dipl.-Ing. degree from the University of Belgrade, Belgrade, Serbia, the Ph.D. degree from Caltech, Pasadena, CA, USA, and the Doktora Honoris Causa (honorary doctorate) degree from Carlos III University, Madrid, Spain. in 2022.

She was a Visiting Professor with the Technical University of Munich, Munich, Ger-



many, from 2001 to 2003; ISAE, Toulouse, France, in 2014; and the Chair of Excellence at Carlos III University from 2018 to 2019. She is currently a Distinguished Professor and the Lockheed Martin Endowed Chair in Electrical Engineering at the University of Colorado Boulder, Boulder, CO, USA. She has graduated over 70 Ph.D. students and currently advises 18 doctoral students. Her research interests are in high-efficiency power amplifiers and transmitters, microwave and millimeter-wave high-performance circuits for communications and radar, medical applications of microwaves, quantum sensing and metrology, and wireless powering.

Dr. Popović was elected as a Foreign Member of the Serbian Academy of Sciences and Arts in 2006. She was elected as a member of the National Academy of Engineering in 2022 and a Fellow of the National Academy of Inventors in 2024. She was a recipient of two IEEE MTT Microwave Prizes for best journal papers, the White House NSF Presidential Faculty Fellow Award, the URSI Issac Koga Gold Medal, the ASEE/HP Terman Medal, and German Alexander von Humboldt Research Award. She was named an IEEE MTT Distinguished Educator in 2013 and the University of Colorado Distinguished Research Lecturer in 2015.

Dipankar Shakya (Graduate Student Member, IEEE) received the B.E. degree in electronics and communications from Tribhuwan University, Kirtipur, Nepal, in 2016, and the M.S. degree in electrical engineering from New York University, New York, NY, USA, in 2021. He is currently working toward the Ph.D. degree in electrical engineering at the NYU Wireless Research Center, Tandon



School of Engineering, New York University, Brooklyn, NY, USA, under the supervision of Prof. Theodore S. Rappaport.

In 2019, he joined the NYU Wireless Research Center, New York University, following three years of service as an Engineer for flood early warning systems in different South Asian countries. His research interests include FR1(C), FR3, millimeter-wave and terahertz radio propagation measurement systems, channel modeling, and radio frequency integrated circuits symposium (RFIC) design.

Jose V. Siles (Senior Member, IEEE) received the Ph.D. degree in electrical engineering from the Technical University of Madrid, Madrid, Spain, in 2008. His Ph.D. dissertation was focused on the physicsbased modeling of semiconductor devices for terahertz applications, and part of this research was performed at the University of Rome "Tor Vergata," Rome, Italy, and the Observatory of Paris-LERMA, Paris, France.



From 2008 to 2010, he was a Postdoctoral Fellow with the Observatory of Paris-LERMA, participating in several programs funded by the CNES, European Space Agency, and European Commission. In 2010, he joined the Submillimeter-Wave Advanced Technology Group, NASA Jet Propulsion Laboratory, California Institute of Technology, Pasadena, CA, USA, as a Fulbright Postdoctoral Fellow. He is currently the Project Manager and the Technical Lead of NASA's ASTHROS mission, which is planned to launch from Antarctica in 2024. His research interests include the design, development, and test of solid-state power-combined multiplied local oscillator sources and receivers for high-resolution multipixel heterodyne cameras at submillimeter-wave and terahertz frequencies for astrophysics, planetary science, and radar imaging applications.

Dr. Siles was a recipient of the Fulbright Postdoctoral Research Award at the NASA Jet Propulsion Laboratory for the term of 2010–2012, the 2012 NASA/JPL Outstanding Postdoctoral Research Award, the 2019 NASA/JPL Lew Allen Award for Excellence, and U.S. Antarctic Service Medal in 2016.

**Theodore S. Rappaport** (Fellow, IEEE) received the Ph.D. degree from Purdue University, West Lafayette, IN, USA, in 1987.

He is currently the David Lee/Ernst Weber Professor with New York University (NYU), New York, NY, USA, and holds faculty appointments at the Department of Electrical and Computer Engineering, NYU Tandon School of Engineering, the Courant Com-



puter Science Department, and the NYU Langone School of Medicine. He is also the Founding Director of the NYU Wireless Research Center, NYU, a multidisciplinary research center focused on the future of wireless communications and applications. His research has led the way for modern wireless communication systems. In 1987, his Ph.D. study provided fundamental knowledge

of indoor wireless channels used to create the first Wi-Fi standard (IEEE 802.11), and he conducted fundamental work that led to the first U.S. Digital cellphone standards, TDMA IS-54/IS-136, and CDMA IS-95. He and his students engineered the world's first public Wi-Fi hotspots, and his work proved the viability of millimeter waves for mobile communications. The global wireless industry adopted his vision for fifth-generation (5G) millimeter-wave cellphone networks. His most recent research has proven the viability of subterahertz wireless communications and position location for 6G, 7G, and beyond. He founded three academic wireless research centers at Virginia Tech, Blacksburg, VA, USA; The University of Texas, and NYU that have produced thousands of engineers and educators since 1990, and he has coauthored over 300 papers and 20 books, including the most cited books on wireless communications, adaptive antennas, wireless simulation, and millimeter-wave communications. He co-founded two wireless companies, TSR Technologies, Blacksburg, and Wireless Valley Communication, Austin, TX, USA, which were sold to publicly traded companies, and he has advised many others. He has more than 100 patents issued and pending. He served on the Technological Advisory Council of the Federal Communications Commission (ECC).

Dr. Rappaport is a member of the National Academy of Engineering and the Wireless Hall of Fame, a Fellow of the Radio Club of America and the National Academy of Inventors, a Life Member of the American Radio Relay League, a Licensed Professional Engineer in Texas and Virginia, and an Amateur Radio Operator (N9NB). He received the IEEE Eric Sumner Award, the ASEE's Terman Award, The Sir Monty Finniston Medal from the Institution of Engineering and Technology (IET), the IEEE Vehicular Technology Society's James R. Evans Avant Garde and Stu Meyer Awards, the IEEE Education Society William E. Sayle Award for achievement in education, the IEEE Communications Society Armstrong Award, and the Armstrong Medal and Sarnoff Citation from the Radio Club of America. He co-founded the Virginia Tech Symposium on Wireless Communications in 1991, the Texas Wireless Summit in 2003, and the Brooklyn 5G Summit (B5GS) in 2014.